This is the accepted version of the following article:

Meloun, M., Pilařová, L., Javůrek, M., & Pekárek, T. (2018). Multiwavelength UV-metric and pH-metric determination of the dissociation constants of the hypoxia-inducible factor prolyl hydroxylase inhibitor Roxadustat. *Journal of Molecular Liquids*, *vol. 268. pp. 386-402. doi:* 10.1016/j.molliq.2018.07.076

This postprint version is available from URI https://hdl.handle.net/10195/72662

Publisher's version is available from

https://www.sciencedirect.com/science/article/pii/S016773221832525X?via%3Dihub

This postprint version is licenced under a Creative Commons Attribution-NonCommercial-NoDerivatives 4.0.International.

Multiwavelength UV-metric and pH-metric determination of the dissociation constants of the hypoxia-inducible factor prolyl hydroxylase inhibitor Roxadustat

*Milan Meloun[1], Lucie Pilařová[1], Milan Javůrek[2] and Tomáš Pekárek[3]
[1]Department of Analytical Chemistry, University of Pardubice, CZ 532 10 Pardubice, Czech Republic,
[2]Department of Process Control, University of Pardubice, CZ 532 10 Pardubice, Czech Republic
[3]Zentiva k.s., U kabelovny 130, CZ 102 37 Prague, Czech Republic
***Corresponding author:** milan.meloun@upce.cz, **Phone:** +420466037026, **Fax:** +420466037068,

Abstract: UV-VIS spectra, molar absorption coefficients and protonation equilibriaRoxadustat is an orally bioavailable, hypoxia-inducible factor prolyl hydroxylase inhibitor with potential anti-anemic activity. It is one of the Active Pharmacenutical Ingredients possessing acidic/basic functionalities their ionization state is controlled by solution pH and acid dissociation constants. Nonlinear regression of the pH-spectra with programs REACTLAB and SQUAD84 and of the pH-titration curve with ESAB determined four multiple consecutive dissociation constants with the protonation scheme. A sparingly soluble neutral molecule LH_3 of Roxadustat was dissociated to the soluble anions LH_2^-, LH^{2-} and L^{3-} or protonated to the cation LH_4^+ in an aqueous medium. The graph of molar absorption coefficients of variously protonated species according to wavelength shows that the spectra of two anions LH_2^- and $LH^{2-}$are nearly the same in colour. The Roxadustat spectrum exhibited five sharp isosbestic points related to the LH^{2-}/L^{3-} equilibrium. Four consecutive thermodynamic dissociation constants were estimated using UV-metric data $pK^T_{a1} = 3.60(04)$, $pK^T_{a2} = 5.62(14)$, $pK^T_{a3} = 7.66(16)$, $pK^T_{a4} = 9.08(02)$ at 25°C and $pK^T_{a1} = 3.60(04)$, $pK^T_{a2} = 5.73(10)$, $pK^T_{a3} = 7.52(10)$, $pK^T_{a4} = 8.99(02)$ at 37°C and using pH-metric data $pK^T_{a1} = 4.33(09)$, $pK^T_{a2} = 6.57(11)$, $pK^T_{a3} = 8.88(05)$, $pK^T_{a4} = 9.03(04)$ at 25°C and $pK^T_{a1} = 4.25(09)$, $pK^T_{a2} = 6.49(10)$, $pK^T_{a3} = 8.80(06)$, $pK^T_{a4} = 9.00(05)$ at 37°C The positive values of the enthalpy ΔH^0 showed that the dissociation process is endothermic and the positive values of the Gibbs free energy ΔG^0 at 25°C indicated that the dissociation process was not spontaneous, which also was confirmed by a negative value of the entropy ΔS^0. Four macro-dissociation constants of Roxadustat and six protonation locations were predicted by MARVIN.

Keywords: Dissociation constants; Roxadustat; spectrophotometric titration; pH-titration; REACTLAB; SQUAD84; ESAB;

Highlights:

- Roxadustat is a second-generation of the prolyl-hydroxylases domain PHD inhibitor
- Protonation equilibria studied using UV-metric and pH-metric titration analysis
- Four close pK^T_{a1}, pK^T_{a2}, pK^T_{a3}, pK^T_{a4} determined at 25ºC and 37ºC in an aqueous medium
- The number of protonated species estimated from the rank of the UV-absorbance matrix
- The ΔH^0, ΔG^0 and ΔS^0 prove the dissociation is endothermic and not spontaneous

Graphical abstract:

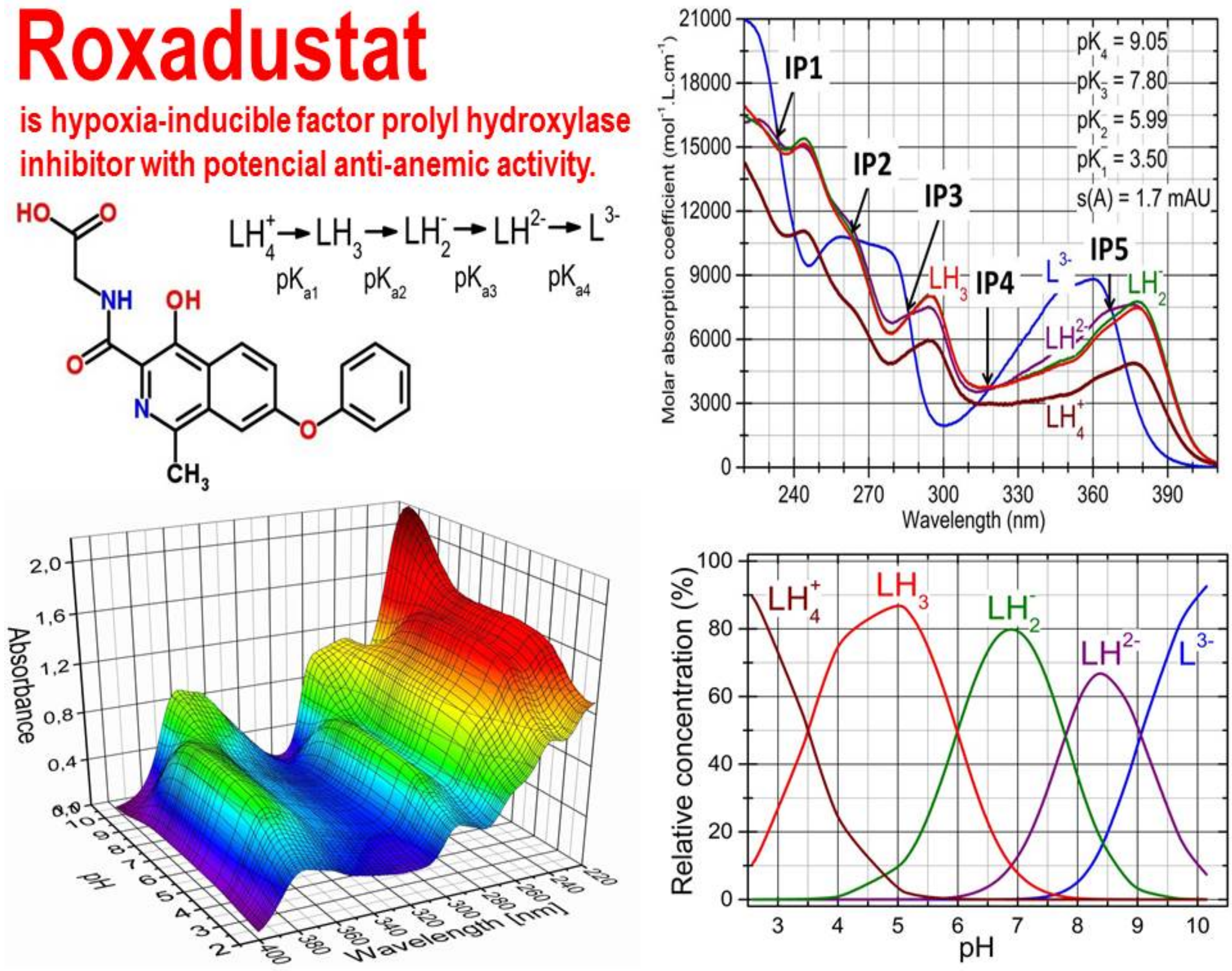

1. Introduction

Anaemia is one of the hallmarks of advanced chronic kidney disease (CKD); it correlates with a lower quality of life and increased cardiovascular risk. The inhibitors of the prolyl-hydroxylases domain (PHD) are oral drugs which activate the hypoxia-inducible factors (HIF) and stimulate the production of endogenous erythropoietin. ***Roxadustat*** (marked FG-4592, ASP1517) is a second-generation prolyl-hydroxylases domain inhibitor; it is currently undergoing now phase-III clinical development [1]. A classic response to hypoxia is an increase in red blood cell production [2-4]. This reaction is controlled by the prolyl hydroxylase/hypoxia-inducible factor (HIF) pathway, which regulates a wide range of cellular functions. The discovery of this pathway as a key regulator of erythropoiesis has led to the development of small molecules that stimulate the production of endogenous erythropoietin and increase iron metabolism. Roxadustat is a hypoxia-inducible stabilizer (HIF) that can increase the number of red blood cells in the body [5,6]. Roxadustat is an orally bioavailable, hypoxia-inducible factor prolyl hydroxylase inhibitor (HIF-PHI) with potential anti-anemic activity [7] [8] [9]. Upon administration, Roxadustat binds to and inhibits HIF-PHI, an enzyme responsible for the degradation of transcription factors in the HIF family under normal oxygen conditions. This prevents HIF breakdown and promotes HIF activity [10,11]. Increased HIF activity leads to an increase in endogenous erythropoietin production, thereby enhancing erythropoiesis [7]. It also reduces the expression of the peptide hormone hepcidin, improves iron availability, and boosts hemoglobin levels [12]. Phase-II clinical trials have shown that Roxadustat is effective and safe in the short term in either non-dialysis or dialysis CKD patients (NDD-CKD). Besarab et al. [13] showed that Roxadustat stimulates erythropoiesis as an oral hypoxia-induced prolyl hydroxylase inhibitor. Roxadustat caused dose-dependent increases in Hb blood in patients with anemic NDD-CKD. Presently, anemia associated with chronic kidney disease (CKD) is being studied as an oral treatment [14,15] [16] [17] [18] [19]. Based on previous studies [20] [21] Roxadustat is able to correct and maintain hemoglobin levels in patients with CKD non-dialysis. Eichner [22] and others [20,22] [23] studied Roxadustat and main plasma- and urine-derived metabolites were investigated in the context of routine doping control analytical approaches. A study [24] in the treatment of anemia associated with chronic kidney disease evaluated the effects of mild hepatic impairment on the pharmacokinetics of Roxadustat, pharmacodynamics and tolerability in patients with normal hepatic function.

IUPAC name of Roxadustat is 2-[(4-hydroxy-1-methyl-7-phenoxyisoquinoline-3-carbonyl)amino]acetic acid marked CODE FG-4592; ASP1517, CAS 808118-40-3. Molecular formula is $C_{19}H_{16}N_2O_5$ and molecular weight 352.106 g/mol. The colour is clear or slightly opalescent, and colorless to pale brown solution in a single-dose vial for injection.

Fig. 1

As the majority of drugs are weak acids or bases, knowledge of the dissociation constant in each case helps in understanding the ionic form of a molecule [25]. Roxadustat belongs to Active Pharmacenutical Ingredients (APIs) which have acidic/basic functionalities, their ionization state is controlled by both solution pH and its acidic dissociation constants pK_a [26]. These different chemical species (cationic, neutral, or anionic) often have vastly different properties with respect to water solubility, volatility, UV absorption, and reactivity with chemical oxidants. The ionized form is usually more water soluble, while the neutral form is more lipophilic and has higher membrane permeability [26]. The pK_a value is a key physicochemical parameter influencing many biopharmaceutical characteristics in pharmacokinetic and bioavailability studies [27-30]. The dissociation constants of a compound influences lipophilicity, solubility, and permeability and play a crucial role in the characterization of its absorption, distribution, metabolism and excretion (ADME) profile [31,25,32-34]**.** Since this drug has been given a great deal of attention over the past two years [1-33], therefore we wanted to introduce the basic physical and chemical parameters such as UV-VIS spectra, molar absorption coefficients, protonation equilibria and corresponding dissociation constants.

Manallack found that the pK_a distributions of drugs are influenced by the nature and frequency of occurrence of the functional groups that are commonly observed in pharmaceuticals. There are several methods for determining dissociation constants. Traditionally, potentiometry [35,36] and UV-VIS absorption spectrophotometry [37] have been the most useful techniques for the determination of equilibrium constants, due to their accuracy and reproducibility. In these methods a physical property of an analyte is measured as a function of the pH of a solution and resulting data are then used for determining dissociation constants. Moreover, pK_a values can also be theoretically predicted by computational methods on the base of molecular structure:

1. Potentiometry, pH-metric titration analysis, a sample is titrated with acid or base using a pH glass electrode to monitor the course of titration. The pK_a value is estimated from the change in the shape of the titration curve compared with that of blank titration without a sample present. Analysis methods commonly used to derive

pK_a´s from titration curves include Gran´s plot [38], second-derivative (Δ^2pH/ΔV^2) [36], and least-squares non-linear regression using ESAB [39] or HYPERQUAD [40,41].

2. Spectrophotometry, and UV-metric spectra analysis [42] in particular, is a highly sensitive and convenient method to determine pK_a in very diluted aqueous solutions since it requires relatively simple equipment and can work with a sub-micromolar compound concentration (about 10^{-5} to 10^{-6} M), *ref.* [26] [43-45]. The main advantage is higher sensitivity (> 10^{-6}M) to compounds with favourable molar absorption coefficients [26]. However, in such a case, a compound must contain a UV-active chromophore close enough to the site of the acid-base function in the molecule. The authors [46-49] have shown that spectrophotometric titration in combination with suitable chemometric tools can be used to determine dissociation constants pK_a even for sparingly soluble drugs [47] [50]. The most relevant algorithms are SQUAD84 [44] and REACTLAB [51]. It is still believed that spectrophotometric data are inherently less precise than potentiometric data [52]; consequently most equilibrium constants are determined by means of pH-metric potentiometric titrations using ESAB [39] or HYPERQUAD [40,41].

3. The accuracy of theoretical pK_a predictions from a molecular structure with two predictive programs ACD/Percepta [53-59] and MARVIN [55,56,60,61,58,62,53,63] was found to be the best of all nine other similar programs.

The aim of our study was to examine the regression analysis of the pH-absorbance matrix with changes in spectra and also to carry out a pH-metric potentiometric determination of the protonation model to find suitable conditions for a reliable regression determination of dissociation constants.

2 Computational details

Spectrophotometric pH-titration data were treated using the program SQUAD84 [44] and REACTLAB [51] with dissociation constants and molar absorptivity spectral profiles and a distribution diagram of the relative concentrations of the pure species by the nonlinear regression of pH-spectra. A detailed tutorial of the UV-metric titration [42], and alternative pH-metric titration has been previously described [47,50].

An ***isosbestic point*** is a specific wavelength at which the total absorbance of a sample does not change during a chemical reaction of the sample. When an isosbestic plot is constructed by the superposition of the absorption spectra of two species whether by using molar absorption coefficients for the representation, or by using absorbance and keeping the same molar concentration for both species, the isosbestic point corresponds to the wavelength at which these spectra cross each other. A pair of substances can have several isosbestic points in their spectra. When a “1-to-1” chemical reaction (one mole of reactant gives one mole of product) including equilibria involves a pair of substances with an isosbestic point, the absorbance of the reaction mixture at this wavelength remains invariant, regardless of the extent of reaction or the position of the chemical equilibrium. This occurs because the two substances absorb light of that specific wavelength to the same extent, and the analytical concentration remains constant. The requirement for an isosbestic point to occur is that the two species involved are related linearly by stoichiometry, such that the absorbance is invariant for one particular wavelength. Thus ratios other than one-to-one are possible (IUPAC [64]).

3 Materials and method

3.1 Materials

Roxadustat hydrochloride donated by ZENTIVA k. s., (Prague) with declared purity checked by a HPLC method and alkalimetrically, was >99%. This drug was weighted straight to a reaction vessel resulting in a concentration of about 8.0×10^{-5} mol. dm^{-3}. Other chemicals have been previously described [47].

3.2 Apparatus

The apparatus used and both titration procedures were described in detail [49,65,48,50]. Absorption spectra were measured with a titration set-up consisting of a computer interfaced to a spectrophotometer GBC CINTRA 4040, GBC Scientific Equipment Pty Ltd., Braeside, Victoria 3195, Australia. The pH values were adjusted in a range of 2.5 to 11.5 using a convenient phosphate buffer and the absorption spectra at 75 pH values were related to each sample. The experimental and computation scheme to determine the dissociation constants of the multi-component system is taken from the book Meloun *et al, cf.* page 226 in *ref.* [66] and all steps were described in details [48]. The free hydrogen-ion activity a_{H+} was measured on the digital voltmeter Hanna HI 3220 with a precision of ±0.002 pH using the combined glass electrode Theta HC 103-VFR. The potentiometric titrations of drugs with potassium hydroxide were performed using a hydrogen activity scale. Standardization of the pH meter was performed using WTW standard buffers values, 4.006 (4.024), 6.865 (6.841) and 9.180 (9.088) at 25°C and 37°C, respectively, in brackets.

3.3 UV-metric procedure

The spectrophotometric multiple-wavelength pH-titration was carried out in two steps. In the first step, the glass pH-electrode system was calibrated. The alkali titer and absence of carbonate were periodically checked by pH-metry, using the appropriate Gran function against primary standard oven-dried potassium hydrogen phthalate. In the second step, a solution of a fully protonated compound (20.0 mL containing 8.0×10^{-5} $mol.dm^{-3}$ Roxadustat) to be analyzed at the required conditions of temperature, ionic strength and solvent composition, was added to the pre-titrated background solution and small amounts of a KOH solution were then added into the reaction vessel. The spectral data were obtained after adding microliters of HCl titrant from the piston microburette to change the pH in the range of 11 – 2. After each HCl titrant addition, the pH was allowed to stabilize and the pa_H value was read. These microliter-amounts of HCl titrant should be small enough to allow the increase of total volume V_0 to be neglected. During spectrophotometric titrations, the test solution was pumped to a spectrophotometric flow-cuvette by a peristaltic pump. After each addition of titrant, and after waiting for the pa_H reading to become stable, the spectra were recorded with 1 nm resolution over the 220 – 410 nm interval to obtain different spectra around the maximum for studied compound.

3.4 pH-metric procedure

Potentiometric determination using the ESAB program [67,39] was previously described. For dissociation reactions realized at constant ionic strength the so-called “mixed dissociation constants pK_a” and the mass balance equations are $L = l + \sum_{j=1}^{J} \beta_{H_j} l h^j$, $H = h - \frac{K_w}{h} + j\sum_{j=1}^{J} \beta_{H_j} l h^j$. It is obtained with a proton-sensitive glass, and the reference electrodes cell can be described by the equation

$$E_{cell} = E^0 + \frac{f.RT\ln 10}{F}\log a_{H^+} + j_a a_{H^+} - \frac{j_b K_W}{a_{H^+}} - E_{ref} = E^{0'} + S\log h \,,$$

where E^{o} is the standard potential of a glass electrode cell containing some other constants of the glass electrode as the asymmetry potential, etc., and $a_{H^+} = \left[\mathrm{H}^+\right] y_{H^+} = h y_{H^+}$, a liquid-junction potential E_j is expressed by the term $E_j = j_a a_{H^+} - j_b K_w / a_{H^+}$, and $S = (f.\ RT \ln 10)/F$ is the slope of glass electrode for a Nernstian response, K_w is the operational ion product of water at temperature T [K], the correction factor f, is taken as an adjustable parameter. Under a constant ionic strength the activity coefficient does not change, and the term $E^{0'}$ in the pa_{H} range from 3 to 11 is practically constant. Under constant ionic strength, dependence is expressed between the volume of *titrant* added from burette V_i and the monitored *emf* $E_{cell,i}$ or p$a_{\mathrm{H+}}$ with the vector of unknown parameters (***b***) being separated into the vector of *common parameters* (***K*$_\mathbf{a}$**) and the vector of *group parameters* (**p**), *i. e.* $V_i = f(E_{cell,i};\mathbf{b}) = f(E_{cell,i};\mathbf{K_a},\mathbf{p})$. The vector of common parameters $\boldsymbol{K}_\mathbf{a}$ = $(K_{a,\ 1},\ \ldots,\ K_{a,\ m})$ contains m dissociation constants of the acid LH$_\mathrm{j}$. The vector of group parameters **p** = $(E^{0'}, S, K_w, j_a, j_b, L_0, L_T, H_0, H_T)$ contains two constants of the Nernstian equation, $E^{0'}$ and S, and also the total ligand concentration, L_0, and the hydrogen ion concentration, H_0 of the titrand in vessel, and the corresponding quantities of titrant, L_T and H_T in burette. Group parameters ***p*** can be refined simultaneously with the common parameters $\boldsymbol{K}_a$. The program ESAB [67,39] is based on a minimization of the sum of squared residuals *RSS*. It uses the strategy for treating *emf* or p$a_{\mathrm{H+}}$ data or the volume of *added titrant V* from burette to find dissociation constants that give the "best" fit to experimental data. As primary data contains the total concentration H_T of proton from burette and the measured p$a_{\mathrm{H+}}$, one could trust p$a_{\mathrm{H+}}$ and minimize the residual sum of squares $(V_{exp} - V_{calc})^2$. The residual e is formulated with the volume of *added titrant V* from burette so that $e_i = (V_{exp,i} - V_{calc,i})$ and the resulting residual sum of squares $U(\boldsymbol{b})$ is defined $U(\mathbf{b}) = \sum_{i=1}^{n} w_i (V_{\exp,i} - V_{calc,i})^2 = \sum_{i=1}^{n} w_i e_i^2$, where w_i is the statistical weight usually set equal to unity.

3.5 Software

An estimation of the dissociation constants was performed by the nonlinear regression analysis of the UV-metric spectra using SQUAD84 [44], REACTLAB [51] programs and potentiometric pH-metric titration data using the ESAB program [67,39], and by spectra interpretation using the INDICES program [68]. Most graphs were plotted using ORIGIN 9.1, ref [69]. ACD/Percepta [53-59] and MARVIN [55,56,60,61,58,62,53,63] programs for predictions of pK_a′s are based on the structural formulae of drug compounds.

4 Results

The methods of analysis of the pH-absorbance response matrix and pH-potentiometric titration curves have proven two of the most convenient instrumental methods, which reliably determined even close consecutive dissociation constants of sparingly soluble drugs. The UV-metric method measured absorbance with respect to changes in pH, leading to changes in the pH-absorbance response surface of the molecule [70] (Fig. 2). There exists one great disadvantage of the UV-metric method: If the compound possesses no pH-active chromophore, then the UV-metric method cannot be applied. The nonlinear regression analysis of spectrophotometric data was an effective and reliable tool, even in the case of small changes in spectra when changing the pH of the chromophore.

4.1 UV-metric spectra analysis

The experimental procedure and computational strategy for determining the dissociation constants by analyzing the pH-absorbance matrix and potentiometric pH-titration has been described by using a 10-steps procedure based on the previously published Tutorial [48]. In a UV-metric titration, the absorbance-response surface represented the series of spectra at adjusted pH values (Fig. 2a). Before any data processing, the spectral data were subjected to a baseline correction procedure to minimize the effects of a non-specific baseline shift usually caused by light scattering (*e.g.*, due to small air bubbles stirred into the light path) and/or by UV light-source intensity fluctuation. The pH-absorbance spectra (Fig. 3a) were recorded with the acid-base titration of 8.0 $\times 10^{-5}$ mol.dm^{-3} Roxadustat alkalized with the KOH to a pH of 11.6 in an aqueous medium of the phosphate buffer with an ionic strength adjusted to 0.1M with KCl and inerting with argon at 25°C and 37°C. The alkalized solution of Roxadustat was then titrated with HCl to pH 2.6. A set of recorded Roxadustat spectra at a pH from 11.6 to 2.6 covering a wavelength range from 220 to 410 nm was identified as *the entire spectrum* (Figs. 2a and 3a).

Fig. 2

Step 1: *Prediction of pK$_a$ from the Roxadustat structure:* The first step of data analysis was the prediction of dissociation constants, having been based on a quantum-chemical calculation and concerned the structural pattern of the studied molecule. The predictive program MARVIN (or ACD/Percenta) indicated six protonizable sites of Roxadustat, marked on Fig. 2c with letters A through F, which could be associated with predicted dissociation constants, *i.e.*, A with $pK_1 = 2.24$, B with $pK_2 = 3.35$, C with $pK_3 = ?$, D with $\mathrm{pK}_4 = 7.59$, E with $\mathrm{pK}_5 = 8.88$, and F with $\mathrm{pK}_6 = 9.76$. An inspection of the Roxadustat chemical structure revealed four basic centers localized on Fig. 2c with letters A, B, D and E, which could be examined spectrophotometrically. The electronic nature of all chromophores differed considerably. Hence, in order to facilitate the prediction of particular protonation/dissociation sites, the whole molecule of Roxadustat was further subdivided on Fig. 2c into three auxiliary fragments 1 – 3. The fragment containing these centers was not affected by the electron field of the rest of molecule, and therefore their predicted pK_a values differed from pK_a values, predicted from the whole Roxadustat molecule [71]. The drug Roxadustat behaved mostly as a neutral molecule LH_3 in an aqueous medium of pH 5 - 6. When this substance was acidified from pH 5 to 2, the cation LH_4^+ was formed. When changing the pH from 6 to 11, three anions LH^-, LH^{2-}, and L^{3-} appeared. The ACD/Percepta program displayed similar predicted values p*K* as were achieved with the MARVIN program.

Fig. 3

Step 2: *Number of light-absorbing species n_c in a solution of Roxadustat:* To build a regression model of all protonation equilibria of Roxadustat, it was first necessary to estimate the number of light-absorbing species n_c. This number helped to establish a true hypothesis of the protonation model. The entire spectrum on Fig. 3a was firstly divided into three sets of spectra (Fig. 3b, 3c, 3d), wherein the first one covered the pH region from pH 2.6 to 4.2, the second one the pH from 4.2 to 8.1 and the third one the pH from 8.2 to 11.6. By changing the pH, the absorbance of a chromophore changed, and this change has to be examined in three pH ranges. (b) Small changes of the absorbance marked in plots Delta A were detected in estimating the pK_1 in the pH range 2.6 - 4.2. (c) A similar case applied in estimating pK_2 and pK_3 in the pH range 4.2 - 8.1. (d) Sufficient big changes of the absorbance occured only in estimating the pK_4 in the range of 8.2 - 11.6. This figure showed that in the range of pH 8.2 - 11.6, the Roxadustat spectrum exhibited five sharp isosbestic points related to the LH^{2-}/L^{3-} equilibrium. In the pH range 4.2 - 8.1 (Fig. 3c), the isosbestic points were not as clear as in the previous pH range 8.2 - 11.6. In acidic pH range 2.6 - 4.2 (Fig 3b) there were small changes in the spectrum at the pH change and the equilibrium LH_3/LH_4^+ was therefore markedly uncertain.

The absorbance matrix ***A*** contains *m* columns of the measured pH values adjusted at *n* wavelength in lines. INDICES algorithm [68] drawed the Cattel´s index graph $s_k(A)$ relative to index *k* (Fig. 3e). The found solution was *k**, which represented a coordinate of the significant break on the curve $s_k(A) = f(k)$. There exist 16 various modifications in program INDICES to this approach related by different authors such as the residual standard deviation RSD, the root mean error square RMS, and others, ref. [42]. The Cattel index graph of eigenvalues (Fig. 3e) showed that the total spectrum of the Roxadustat at the wavelengths of 220 - 410 nm indicated five light-absorbing species. This graph on the semilogarithmic scale led to the same conclusion (Fig. 3f). This means that four dissociation constants were preferred and five species LH_4^+, LH_3, LH_2^-, LH^{2-} and L^{3-} were supposed to be present in the equilibrium mixture.

Fig. 4

Step 3: *Diagnostics for the search of the protonation model building and testing:* The hard modeling technique SQUAD84 and soft-modeling technique REACTLAB were used for protonation model building. In both programs the same computational strategy was applied, *i. e.,* the *regression triplet* (criticism of data, model and method), *cf.* ref. [46,72]. The residuals-least-squares method *RSS* quantified the sum of the residuals of the absorbances between the experimental and calculated spectra. The calculated spectrum was enumerated as the sum of the contributions of all differently protonated species, when their concentrations were calculated for the estimated dissociation constants. In an iterative process, the molar absorption coefficients of all of these species were estimated. The search for the best hypothesis of the protonation model were supposed to contain two, three or four three dissociation constants as shown on Fig. 4. This contained the graphs of the molar absorption coefficients and the distribution diagrams of all the species acquired from three tested hypotheses of the protonation model. The reliable criterion for the best hypothesis is based on the resulting goodness-of-fit test of the calculated spectra through the experimental points of the absorbance matrix $s(A)$. The best fitness of experimental spectra set was achieved for the hypothesis of five differently protonated species LH_4^+, LH_3, LH_2^-, LH^{2-} and L^{3-}. For the tested hypothesis of the protonation model starting with three dissociation constants, there was little difference in the shape of the spectral curves of the molar absorption coefficients ε = f (λ) for two differently protonated anions LH^{2-} and LH_2^-, which were difficult to distinguish from each other. A similar situation occurred in the next tested protonation hypothesis of four dissociation constants, where it was difficult to distinguish the □ = f (λ) curves of three anions LH^{2-} relative to LH_2^- and to molecule LH_3. Only the curves of cation LH_4^+ and anion L^{3-} were clearly separated. The standard deviation of the absorbance $s(A)$ reached the lowest value for the most probable hypothesis of the four dissociation constants and was conveniently used as the most reliable criterion of the fitted regression model.

Table 1

The estimates of the dissociation constants using two regression programs, SQUAD84 and REACTLAB, were compared in Table 1. The mean residual $E|e|$ [mAU], the standard deviation of residuals $s(e)$ [mAU] and the Hamilton *R-factor* of relative fitness [%] in SQUAD84 showed that an excellent fit of the calculated spectra was achieved for the protonation model with four dissociation constants. REACTLAB seemed to offer the more reliable parametric estimates as it always reached a better curve fitting than the independent program SQUAD84. The reliability of the regression parameter estimates might be tested using the following general diagnostics (Table 1 and Fig. 4) as they have been previously introduced in ref. [48]:

(a) *The physical meaning of parametric estimates.* In the left part of Fig. 4 the estimated molar absorptivities of all of the variously protonated species □$_{L}$, □$_{LH}$, □$_{LH2}$, □$_{LH3}$ and □$_{LH4}$ of Roxadustat on wavelength were shown.

(b) *The physical meaning of the species concentrations.* The distribution diagram (Fig. 4) showed the protonation equilibria of LH_4^+, LH_3, LH_2^-, LH^{2-} and L^{3-}. At pH 5 Roxadustat is in the form of the neutral molecule LH_3. An acidification of the species LH_3 first creates the cation LH_4^+, while its alkalization leads to anions LH_2^-, LH^{2-} and L^{3-}.

(c) *Goodness-of-fit test:* Although the statistical analysis of residuals [48] gives the most rigorous test of the goodness-of-fit, realistic empirical limits should be respected. The statistical measures of the curve-fitting, *i.e.* the statistical analysis of residuals *e* proved that the minimum of the elliptic hyperparaboloid *RSS* has been reached (Table 1). It means that the mean residual $E|\bar{e}|$ [mAU] and the standard deviation of residuals $s(\hat{e})$ [mAU] always had sufficiently low values, lower than 2 mAU, which was less than 0.2% of the measured absorbance value proving in this way a good fitness. The good fitness achieved also was proven by the small value of the Hamilton *R-factor* mostly less than 0.5%.

Fig. 5

Fig. 5 shows that Roxadustat exhibited the entire spectrum within the UV range of 220 – 410 nm, which could be distinguished in five absorption bands with five isosbestic points. The positions of the isosbestic points were also shown in the graph of the molar absorption coefficients vs. wavelength for variously protonated Roxadustat in Fig. 5b. Isosbestic points mainly concerned the equilibrium of anions LH^{2-}/L^{3-}, while the spectrum of other protonated equilibria here only disturbed the detection of the intersection of the spectra of these two species at the isosbestic point (Fig. 5a). For this reason, the detection of five isosbestic points for the anions LH^{2-}/L^{3-} equilibrium in the pH range of 9 - 11 was found as the sharpest. If a third one was partaking in the process, the spectra would typically intersect at *varying* wavelengths as the concentrations change, creating the impression that the isosbestic point was 'out of focus', or it would shift as the conditions changed. The reason for this was that it would be very unlikely for three compounds to have extinction coefficients linked in a linear relationship by chance for one particular wavelength (Fig. 5a). The wavelength of the isosbestic point determined did not depend on the concentration of the substance used, and so it became a very reliable reference of one equilibrium. Contrary to a widely accepted idea, the existence of an isosbestic point did not prove that the reaction was a quantitative conversion of one species into another unique species or that an equilibrium existed only between only two species [64].

Fig. 6

Step 4: *The experimental strategy of an efficient choice of the wavelength range:* In equilibria study it was convenient to examine the dependence of the proximity between the ionisable group and the chromophore, as the spectral shift might not have been strong enough to allow for a successful determination of dissociation constants. It was important to select the wavelength range to assess the effect of the ionizable center on chromophore when changing pH. All absorption bands differed in sensitive chromophores to pH change, so it was necessary to compare the dissociation constants estimated from the entire spectrum of wavelength A - D in Fig. 6 with those estimated from three separate absorption bands for suggested model of 3 or 4 dissociation constants. Three wavelengths ranges of 220 – 270 nm, 260 – 320 nm, and 320 – 410 nm were selected for regression analysis and the spectra were evaluated. Fig. 6 showed the estimates of dissociation constants including the achieved goodness-of-fit value $s(A)$, which served as the criterion of reliability for the obtained estimates. The best fitness was achieved in the wavelength range 260 – 320 nm, although the dissociation constant estimates were nearly the same in all three ranges.

Fig. 7

The change of pH did not cause the same changes in Roxadustat spectrum because some chromophores were only slightly affected by a pH change. Fig. 7a presented an option of six various wavelengths A through F at which A-pH curves were recorded. Fig 7b showed the distribution diagram of the relative concentration of all variously protonated species on pH. Supposing the protonation model of four dissociation constants, there were analysed the absorbance-pH curves at various wavelengths in actual absorbance units in six graphs A through F which demonstrated a sensitivity of chromophores in Roxadustat molecule on pH changes. The shape of A-pH curves at different wavelengths indicated whether the change in pH caused a sufficient change in absorbance, and whether it was even possible to estimate the actual dissociation constant from this absorbance change. The changes of A-pH curve shape in graphs A through F also contained the positions of the individual dissociation constants $\mathrm{p}K_{\mathrm{a}1}$ to $\mathrm{p}K_{\mathrm{a}4}$ and the corresponding differently protonated species. From the distribution diagram of all protonated species depending on the pH, it was obvious that the protonated equilibrium concerned close and overlapping dissociation constants because the difference between two successive $\mathrm{p}K_{\mathrm{a}}$ was always less than 3. An estimation of the close equilibrium constants was generally always more difficult and required a reliable regression software. Each graph in Fig. 7 also contained a plot of residuals. The quality of residuals revealed the degree of curve fitness of the calculated A-pH curve through the experimental absorbance points. The residuals should oscillate around the zero and their +/- sign should change with their frequent oscilations. The residuals should also exhibit a

Gaussian distribution with a mean value nearly equal to zero. The standard deviation should be of the same size as the instrumental noise, $s_{\mathrm{inst}}(A)$.

Fig. 8

Step 5: *Reproducibility of pK_a estimates for the searched protonation model:* The reproducibility of the dissociation constants of Roxadustat estimated by programs SQUAD84 and REACTLAB from five reproduced measurements were found to be in good agreement at 25°C (Table 1, Fig. 8). The reproducibility of the protonation model estimates concerning three and four dissociation constants was compared, calculated by the spectrophotometric UV-metric method and the potentiometric pH-metric method at 25°C. The arithmetic mean of all reproduced dissociation constants together with its standard deviation was presented. Obtained results of the two hypotheses of protonated model concerning three and four dissociation constants were considered. For the reliability criterion of the hypothesis in question, the fitness test of the calculated spectra, expressed by the standard deviation of an absorbance $s(A)$ or the fitness test of the calculated pH-titration curves by the experimental titration points was expressed as the standard deviation of the titrant volume $s(V)$ in the pH-metric method. Both instrumental methods lead to the conclusion that better curve-fitting was achieved for the protonation model of four dissociation constants.

Fig. 9

Step 6: *Signal-to-noise ratio of the absorbance changes in spectra*: The spectrophotometric determination of $\mathrm{p}K_{\mathrm{a}}$ of the Roxadustat required an investigation into whether the change in pH would cause a sufficient change in absorbance in the spectrum shape. To check the spectral response on the chromophore in the Roxadustat molecule (Fig. 9a and 9b), it was necessary to test whether it was possible to estimate the dissociation constants from the actual spectral changes. The absorbance change Δ_{ij} for the i-th spectrum and the j-th absorbance point of the spectrum could be expressed as $\Delta_{ij} = A_{ij} - A_i$, where the A_i stood for the absorbance of the acid form of Roxadustat. It was necessary to investigate whether these absorbance changes Δ in spectra were sufficiently larger than the size of the instrumental noise $s_{\mathrm{inst}}(A)$ or than the size of the residuals in the mAU units. The absorbance changes Δ in spectra were plotted against the wavelength λ for all absorbance matrix elements (Fig. 9c) to show that even though these values are small they are still larger than the instrumental noise or than the residuals (Fig. 9d). While residuals were in the range (-10 mAU, 8 mAU), the absorbance changes Δ were in the range (-220 mAU, 500 mAU). Therefore, variations in the spectra also influenced the degree of uncertainty of the estimates of the dissociation constants. However, the empirical rule should be kept in mind that if the absorbance changes Δ were less than ±10 mAU, the number of light-absorbing species n_c does not necessarily have to be correctly determined by the factor analysis in INDICES algorithm [68].

Fig. 10

Step 7: *The deconvolution of spectra:* Decomposition of each experimental spectrum into spectra of the individual species proved whether the experimental design was sufficiently efficient. In pH ranges where more components contribute significantly to the spectrum, several spectra should be measured. Such a spectrum provided sufficient information for a regression analysis which monitored at least two species in equilibrium where none of them represented a minor species. Fig. 10 contains six figures of the deconvolution of each measured spectrum into the absorption bands of the variously protonated Roxadustat species. The consecutive deprotonation response in spectra of Roxadustat was demonstrated. At lower pH than 3.5, an absorption band of the cation LH_4^+ was indicated in the equilibrium mixture accompanying the neutral molecule LH_3. From pH 3.5 to pH 6 the absorption band of molecule LH_3 dominated as its concentration increased and the absorption bands of cation LH_4^+ disappeared. From pH 6 to pH 8, the absorption band of anion LH_2^- prevailed as its concentration dominated while from pH 7.5 the concentration of the anion LH^{2-} increased. From pH 9 to pH 11 the anion LH_2^- decreased and only the anion L^{3-} was present.

4.2 pH-metric data analysis

The potentiometric titration of an alkalized mixture of Roxadustat with HCl concerning the pH-metric data analysis was carried out at 25°C and 37°C for an adjusted ionic strength. The initial tentative values of the dissociation constants of the Roxadustat were refined by the ESAB program.

Fig. 11, Table 2

Step 7: *Analysis of pH-metric data and Bjerrum's formation function:* Since Roxadustat could exhibit three or four dissociation constants, their numerical estimation was carried out with the use of the computer-assisted nonlinear regression of the pH-metric titration by the ESAB program. The titration curve concerned alkalized Roxadustat titrated with hydrochloric acid (Fig. 11). The estimates of three and four dissociation constants were evaluated on the graph of the Bjerrum formation curve. However, at a higher concentration than 1 × 10^{-3} mol.dm^{-3} a precipitate of Roxadustat occured which initially formed a slight opalescence.

The ESAB residuals were defined as the difference between the experimental and calculated titrant volume $e_i = V_{exp,\, i} - V_{calc,\, I}$ and were plotted for the model of 3 (Fig. 11c) and 4 (Fig. 11d) dissociation constants. The goodness-of-fit test was carried out with the statistical analysis of residuals. When further group parameters were also refined, the fit was always improved. A quite sensitive criterion for the reliability of the best protonation model tested was the mean of absolute values of residuals $E|\bar{e}|$ = 0.0002 mL. Comparing residuals with the instrumental noise, $s_{\mathrm{inst}}(V)$, represented here by either $s_{\mathrm{inst}}(V) = s(V) = 0.0001$ mL, an excellent fit was confirmed since the mean $E|\bar{e}|$ [mL] and also the residual standard deviation $s(\hat{e})$ = 0.0002 mL were nearly the same for the model of 4 dissociation constants, while for 3 dissociation constants the $s(\hat{e})$ was 0.0090 mL. All residuals oscillated between the lower -0.0002 mL and upper limit 0.0002 mL of Hoaglins inner bounds for 4 dissociation constants and therefore no outlying residuals were indicated outside these bounds (*cf.* page 80 in ref. [73]). The estimate of the best protonation model with 4 dissociation constants estimated by ESAB seems to be quite reliable (Table 2). The curve-fitness was always improved using the refinement of the group parameter L_0 and the actual concentration of the titrated drug Roxadustat.

Fig. 12

Step 9: *Thermodynamic dissociation constants:* Applying a Debye-Hückel equation to the data of Table 1 and 2 the thermodynamic dissociation constants p$K^{\mathrm{T}}_{\mathrm{a}}$ have been estimated at two temperatures 25°C and 37°C. Because of the narrow range and small values of ionic strength, the ion-size parameter *å* and the salting-out coefficient *C* were not estimated. Fig. 12 showed the extrapolation of the mixed dissociation constants to the zero value of an ionic strength according to the limited Debye-Hückel law for four dissociation constants at 25^{0}C and 37^{0}C using UV-metric data (Fig. 12a, b) pK^T_{a1} = 3.60(04), pK^T_{a2} = 5.62(14), pK^T_{a3} = 7.66(16), pK^T_{a4} = 9.08(02) at 25°C and pK^T_{a1} = 3.60(04), pK^T_{a2} = 5.73(10), pK^T_{a3} = 7.52(10), pK^T_{a4} = 8.99(02) at 37°C and using pH-metric data (Fig. 12c, d) pK^T_{a1} = 4.33(09), pK^T_{a2} = 6.57(11), pK^T_{a3} = 8.88(05), pK^T_{a4} = 9.03(04) at 25°C and pK^T_{a1} = 4.25(09), pK^T_{a2} = 6.49(10), pK^T_{a3} = 8.80(06), pK^T_{a4} = 9.00(05) at 37°C. The Working-Hotelling confidence bands expressed the uncertainty of the each dissociation constant estimate, since the broader band is of more uncertain pK_a.

Table 3

Step 10: *Determination of enthalpy and entropy change:* The enthalpy change (ΔH^0) for the dissociation process was calculated using the van't Hoff equation $d\ln K/dT = \Delta H^0/RT^2$. From the Gibbs free-energy change ΔG^0 and enthalpy change ΔH^0 values, the entropy ΔS^0 could be calculated: $\Delta G^0 = -RT \ln K$ and $\Delta S^0 = (\Delta H^0 - \Delta G^0)/T$, where R (ideal gas constant) = 8.314 J.K^{-1}.mol^{-1}, K is the thermodynamic dissociation constant, and T is the absolute temperature. Thermodynamic parameters ΔH^0 and ΔG^0 have been determined from the temperature variation of dissociation constants using the van't Hoff's equation (Table 3).

The positive values of enthalpy ΔH^0(pK_{a1}), ΔH^0(pK_{a2}), ΔH^0(pK_{a3}), ΔH^0(pK_{a4}) show the dissociation process is endothermic. Positive values of ΔG^0(pK_{a1}), ΔG^0(pK_{a2}), ΔG^0(pK_{a3}), ΔG^0(pK_{a4}) at 25°C indicate that the dissociation process is not spontaneous, which was confirmed by a negative value of entropy ΔS^0(pK_{a1}), ΔS^0(pK_{a2}), ΔS^0(pK_{a3}), ΔS^0(pK_{a4}).

Scheme 1

4. Conclusion

1) Roxadustat is one of the Active Pharmacenutical Ingredients (APIs) that have acidic/basic functionalities; their ionization state is controlled by pH and its pK_a.

2) In the range of pH 2 to 11 four dissociation constants could be reliably estimated from the spectra when the concentration of Roxadustat is about 8.0 × 10^{-5} mol.dm^{-3}. Although the somewhat less affected pH changes in the chromophore, four thermodynamic dissociation constants could be reliably determined with SQUAD84 and REACTLAB reaching the similar values with both programs, pK^T_{a1} = 3.60(04), pK^T_{a2} = 5.62(14), pK^T_{a3} = 7.66(16), pK^T_{a4} = 9.08(02) at 25°C and pK^T_{a1} = 3.60(04), pK^T_{a2} = 5.73(10), pK^T_{a3} = 7.52(10), pK^T_{a4} = 8.99(02) at 37°C (Fig. 11a,b).

3) The sparingly soluble neutral molecule LH_3 of Roxadustat was capable of protonation to form the soluble cation LH_4^+ in pure water. The molecule LH_3 could dissociate to anions LH_2^-, LH^{2-} and L^{3-}. The graph of molar absorption coefficients of variously protonated species according to wavelength shows that the spectra of species LH_2^- and $LH^{2-}$are nearly the same in colour. The Roxadustat spectrum exhibited five sharp isosbestic points, which were related to the LH^{2-}/L^{3-} equilibrium.

4) It is still believed that spectrophotometric data are inherently less precise than potentiometric data. The best fitness of experimental spectra set was achieved for the hypothesis of five differently protonated species LH_4^+, LH_3, LH_2^-, LH^{2-} and L^{3-}. There was little difference in the shape of the spectral curves of the molar absorption coefficients $\varepsilon = f(\lambda)$ for two differently protonated anions LH^{2-} and LH_2^-, which were difficult to distinguish from each other.

5) Four thermodynamic dissociation constants of Roxadustat in a potentiometric concentration of 1.0 × 10^{-3} mol. dm^{-3} were determined by the regression analysis of potentiometric titration curves using ESAB, pK^{T}_{a1} = 4.33(09), pK^{T}_{a2} = 6.57(11), pK^{T}_{a3} = 8.88(05), pK^{T}_{a4} = 9.03(04) at 25°C and pK^{T}_{a1} = 4.25(09), pK^{T}_{a2} = 6.49(10), pK^{T}_{a3} = 8.80(06), pK^{T}_{a4} = 9.00(05) at 37°C (Fig. 11c,d).

6) The goodness-of-fit proved sufficient reliability of the parameter estimates of four dissociation constants of the Roxadustat at 25°C and 37°C (Scheme 1). This test was expressed for UV-metric titration by the standard deviation of an absorbance $s(A)$ or for pH-metric titration as the standard deviation of the titrant volume $s(V)$. Both instrumental methods have led to the conclusion that better curve-fitness was achieved for the protonation model of four dissociation constants.

7) Prediction of the dissociation constants of Roxadustat was carried out using the MARVIN and ACD/Percepta programs to specify protonation locations. In comparing two predictive and two experimental techniques, it may be concluded that the prediction programs sometimes vary in estimating pK_a.

8) The values of the enthalpy change ΔH^0 show that the dissociation process is endothermic. Positive values of the Gibbs free energy ΔG^0 at 25°C indicate that the dissociation process is not spontaneous, which was confirmed by a negative value of the entropy ΔS^0.

6. Literature cited

1. Del Vecchio, L., Locatelli, F.: Roxadustat in the treatment of anaemia in chronic kidney disease. Expert Opinion on Investigational Drugs **27**, 125-133 (2018)
2. Haase, V.H.: HIF-prolyl hydroxylases as therapeutic targets in erythropoiesis and iron metabolism. Hemodialysis international. International Symposium on Home Hemodialysis **21 Suppl 1**, S110-S124 (2017)
3. Jain, I.H., Zazzeron, L., Goli, R., Alexa, K., Schatzman-Bone, S., Dhillon, H., Goldberger, O., Peng, J., Shalem, O., Sanjana, N.E., Zhang, F., Goessling, W., Zapol, W.M., Mootha, V.K.: Hypoxia as a therapy for mitochondrial disease. Science **352**(6281), 54-61 (2016)
4. Seeley, T.W., Sternlicht, M.D., Klaus, S.J., Neff, T.B., Liu, D.Y.: Induction of erythropoiesis by hypoxia-inducible factor prolyl hydroxylase inhibitors without promotion of tumor initiation, progression, or metastasis in a VEGF-sensitive model of spontaneous breast cancer. Hypoxia **5**, 1-9 (2017)
5. Hansson, A., Thevis, M., Cox, H., Miller, G., Eichner, D., Bondesson, U., Hedeland, M.: Investigation of the metabolites of the HIF stabilizer FG-4592 (roxadustat) in five different in vitro models and in a human doping control sample using high resolution mass spectrometry. J Pharm Biomed Anal **134**, 228-236 (2017)
6. Hoppe, G., Yoon, S., Gopalan, B., Savage, A.R., Brown, R., Case, K., Vasanji, A., Chan, E.R., Silver, R.B., Sears, J.E.: Comparative systems pharmacology of HIF stabilization in the prevention of retinopathy of prematurity. Proc Natl Acad Sci U S A **113**(18), E2516-2525 (2016)
7. Becker, K., Saad, M.: A New Approach to the Management of Anemia in CKD Patients: A Review on Roxadustat. Advances in Therapy **34**(4), 848-853 (2017)
8. Forristal, C.E., Levesque, J.P.: Targeting the hypoxia-sensing pathway in clinical hematology. Stem cells translational medicine **3**(2), 135-140 (2014)
9. Chen, N., Qian, J., Chen, J., Yu, X., Mei, C., Hao, C., Jiang, G., Lin, H., Zhang, X., Zuo, L., He, Q., Fu, P., Li, X., Ni, D., Hemmerich, S., Liu, C., Szczech, L., Besarab, A., Neff, T.B., Peony Yu, K.H., Valone, F.H.: Phase 2 studies of oral hypoxia-inducible factor prolyl hydroxylase inhibitor FG-4592 for treatment of anemia in China. Nephrology, dialysis, transplantation : official publication of the European Dialysis and Transplant Association - European Renal Association **32**(8), 1373-1386 (2017)

10. Beck, J., Henschel, C., Chou, J., Lin, A., Del Balzo, U.: Evaluation of the Carcinogenic Potential of Roxadustat (FG-4592), a Small Molecule Inhibitor of Hypoxia-Inducible Factor Prolyl Hydroxylase in CD-1 Mice and Sprague Dawley Rats. International journal of toxicology **36**(6), 427-439 (2017)
11. Buisson, C., Marchand, A., Bailloux, I., Lahaussois, A., Martin, L., Molina, A.: Detection by LC-MS/MS of HIF stabilizer FG-4592 used as a new doping agent: Investigation on a positive case. J Pharm Biomed Anal **121**, 181-187 (2016)
12. Besarab, A., Chernyavskaya, E., Motylev, I., Shutov, E., Kumbar, L.M., Gurevich, K., Chan, D.T., Leong, R., Poole, L., Zhong, M., Saikali, K.G., Franco, M., Hemmerich, S., Yu, K.H., Neff, T.B.: Roxadustat (FG-4592): Correction of Anemia in Incident Dialysis Patients. Journal of the American Society of Nephrology : JASN **27**(4), 1225-1233 (2016)
13. Besarab, A., Provenzano, R., Hertel, J., Zabaneh, R., Klaus, S.J., Lee, T., Leong, R., Hemmerich, S., Yu, K.H., Neff, T.B.: Randomized placebo-controlled dose-ranging and pharmacodynamics study of roxadustat (FG-4592) to treat anemia in nondialysis-dependent chronic kidney disease (NDD-CKD) patients. Nephrology, dialysis, transplantation : official publication of the European Dialysis and Transplant Association - European Renal Association **30**(10), 1665-1673 (2015)
14. Del Vecchio, L., Locatelli, F.: Roxadustat in the treatment of anaemia in chronic kidney disease. Expert Opin Investig Drugs **27**(1), 125-133 (2018)
15. Groenendaal-van de Meent, D., den Adel, M., Rijnders, S., Krebs-Brown, A., Kerbusch, V., Golor, G., Schaddelee, M.: The Hypoxia-inducible Factor Prolyl-Hydroxylase Inhibitor Roxadustat (FG-4592) and Warfarin in Healthy Volunteers: A Pharmacokinetic and Pharmacodynamic Drug-Drug Interaction Study. Clin Ther **38**(4), 918-928 (2016)
16. Li, W., Zhao, Y., Fu, P.: Hypoxia Induced Factor in Chronic Kidney Disease: Friend or Foe? Frontiers in medicine **4**, 259 (2017)
17. Locatelli, F., Fishbane, S., Block, G.A., Macdougall, I.C.: Targeting Hypoxia-Inducible Factors for the Treatment of Anemia in Chronic Kidney Disease Patients. American journal of nephrology **45**(3), 187-199 (2017)
18. Mokas, S., Lariviere, R., Lamalice, L., Gobeil, S., Cornfield, D.N., Agharazii, M., Richard, D.E.: Hypoxia-inducible factor-1 plays a role in phosphate-induced vascular smooth muscle cell calcification. Kidney international **90**(3), 598-609 (2016)
19. Schmid, H., Jelkmann, W.: Investigational therapies for renal disease-induced anemia. Expert Opin Investig Drugs **25**(8), 901-916 (2016)
20. Beuck, S., Schanzer, W., Thevis, M.: Hypoxia-inducible factor stabilizers and other small-molecule erythropoiesis-stimulating agents in current and preventive doping analysis. Drug Test Anal **4**(11), 830-845 (2012)
21. Yang, Y., Yu, X., Zhang, Y., Ding, G., Zhu, C., Huang, S., Jia, Z., Zhang, A.: Hypoxia-inducible factor prolyl hydroxylase inhibitor roxadustat (FG-4592) protects against cisplatin-induced acute kidney injury. Clinical science **132**(7), 825-838 (2018)
22. Eichner, D., Van Wagoner, R.M., Brenner, M., Chou, J., Leigh, S., Wright, L.R., Flippin, L.A., Martinelli, M., Krug, O., Schanzer, W., Thevis, M.: lmplementation of the prolyl hydroxylase inhibitor Roxadustat (FG-4592) and its main metabolites into routine doping controls. Drug Test Anal **9**(11-12), 1768-1778 (2017)
23. Saigusa, D., Suzuki, N., Matsumoto, Y., Umeda, K., Tomioka, Y., Koshiba, S., Yamamoto, M.: Detection of novel metabolite for Roxadustat doping by global metabolomics. Journal of biochemistry (2018)
24. Groenendaal-van de Meent, D., Adel, M.D., Noukens, J., Rijnders, S., Krebs-Brown, A., Mateva, L., Alexiev, A., Schaddelee, M.: Effect of Moderate Hepatic Impairment on the Pharmacokinetics and Pharmacodynamics of Roxadustat, an Oral Hypoxia-Inducible Factor Prolyl Hydroxylase Inhibitor. Clinical drug investigation **36**(9), 743-751 (2016)
25. Manallack, D.T.: The pK(a) Distribution of Drugs: Application to Drug Discovery. Perspect Medicin Chem **1**, 25-38 (2007)

26. Babič, S., Horvat, A.J.M., Pavlovič, D.M., Kaštelan-Macan, M.,: Determination of pKa values of active pharmaceutical ingredients. Trends in Analytical Chemistr **26**(11) (2007)
27. Pathare, B., Tambe, V., Patil, V.: A review on various analytical methods used in determination of dissociation constant. International Journal of Pharmacy and Pharmaceutical Sciences **6**(8), 26-34 (2014)
28. Reijenga, J., Hoof, A.v., Loon, A.v., Teunissen, B.: Development of Methods for the Determination of pKa Values. Anal. Chem. Insights **8**, 53-71 (2013)
29. Hernández, J.A., Hernández, A.R., Urbina, E.M.C., Rodríguez, I.M.D.L.G., Manzanares, M.V., Medina-Vallejo, L.F.: New chemometric strategies in the spectrophotometric determination of pKa. European Journal of Chemistry **5**(1), 1-5 (2014)
30. Shayesteh, T.H., Radmehr, M., Khajavi, F., Mahjub, R.: Application of chemometrics in determination of the acid dissociation constants (pK(a)) of several benzodiazepine derivatives as poorly soluble drugs in the presence of ionic surfactants. Eur J Pharm Sci **69**, 44-50 (2015)
31. Pandey, M.M., Jaipal, A., Kumar, A., Malik, R., Charde, S.Y.: Determination of pK(a) of felodipine using UV-Visible spectroscopy. Spectrochim Acta A **115**, 887-890 (2013)
32. Milletti, F., Storchi, L., Sforna, G., Cruciani, G.: New and original pKa prediction method using grid molecular interaction fields. J. Chem. Inf. Model. **47**, 2172-2181 (2007)
33. Settimo, L., Bellman, K., Knegtel, R.A.: Comparison of the accuracy of experimental and predicted pKa values of basic and acidic compounds. Pharm. Res. **31**, 1082-1095 (2014)
34. Tam, K.Y., Takacs-Novak, K.: Multiwavelength spectrophotometric determination of acid dissociation constants: A validation study. Anal. Chim. Acta **434**, 157-167 (2001)
35. Wróbel, R., Chmurzynski, L.: Potentiometric pKadetermination of standard substancesin binary solvent systems. Analytica Chimica Acta **405**, 6 (2000)
36. Qiang, Z., Adams, C.: Potentiometric determination of acid dissociation constants (pKa) for human and veterinary antibiotics. Water Research **38**(12), 16 (2004)
37. Beltran, J.L., Sanli, N., Fonrodona, G., Baron, D., Ozkan, G., Barbosa, J.,: Spectrophotometric, potentiometric and chromatographic pKa values of polyphenolic acids in water and acetonitrile–water media. Anal. Chim. Acta **484**, 12 (2003)
38. Andrasi, M., Buglyo, P., Zekany, L., Gaspar, A.,: A comparative study of capillary zone electrophoresis and pH-potentiometry for determination of dissociation constants. J Pharm Biomed Anal. **44**(5), 8 (2007)
39. De Stefano, C., Princi, P., Rigano, C., Sammartano, S.: Computer analysis of equilibrium data in solution ESAB2M: an improved version of the ESAB program. Annali Di Chimica **77**(7-8), 643-675 (1987)
40. Gans, P., Sabatini, A., Vacca, A.: Investigation of equilibria in solution. Determination of equilibrium constants with the HYPERQUAD suite of programs. Talanta **43**(10), 1739-1753 (1996)
41. Gans, P., Sabatini, A., Vacca, A.: Hyperquad computer-program suite. Abstr Pap Am Chem S **219**, U763-U763 (2000)
42. Allen, R.I., Box, K.J., Comer, J.E.A., Peake, C., Tam, K.Y.: Multiwavelength spectrophotometric determination of acid dissociation constants of ionizable drugs. Journal of Pharmaceutical and Biomedical Analysis **17**(4-5), 699-712 (1998)
43. Hartley, F.R., Burgess, C., Alcock, R.M.: Solution Equilibria. Ellis Horwood, Chichester (1980)
44. Leggett, D.J., McBryde, W.A.E.: General computer program for the computation of stability constants from absorbance data. Analytical Chemistry **47**(7), 1065-1070 (1975)
45. Kankare, J.J.: Computation of equilibrium constants for multicomponent systems from spectrophotometric data. Analytical Chemistry **42**(12), 1322-1326 (1970)
46. Meloun, M., Ferenčíková, Z., Javůrek, M.: Reliability of dissociation constants and resolution capability of SQUAD(84) and SPECFIT/32 in the regression of multiwavelength spectrophotometric pH-titration data. Spectrochim Acta A Mol Biomol Spectrosc **86**, 305-314 (2012)

47. Meloun, M., Nečasová, V., Javůrek, M., Pekárek, T.: The dissociation constants of the cytostatic bosutinib by nonlinear least-squares regression of multiwavelength spectrophotometric and potentiometric pH-titration data. Journal of Pharmaceutical and Biomedical Analysis **120**, 158-167 (2016)
48. Meloun, M., Bordovská, S., Syrový, T., Vrána, A.: Tutorial on a chemical model building by least-squares non-linear regression of multiwavelength spectrophotometric pH-titration data. Anal Chim Acta **580**(1), 107-121 (2006)
49. Meloun, M., Bordovská, S., Vrána, A.: The thermodynamic dissociation constants of the anticancer drugs camptothecine, 7-ethyl-10-hydroxycamptothecine, 10-hydroxycamptothecine and 7-ethylcamptothecine by the least-squares nonlinear regression of multiwavelength spectrophotometric pH-titration data. Anal Chim Acta **584**(2), 419-432 (2007)
50. Meloun, M., Pilarova, L., Pekarek, T., Javurek, M.: Overlapping pK(a) of the Multiprotic Hemostyptic Eltrombopag using UV-Vis Multiwavelength Spectroscopy and Potentiometry. J Solution Chem **46**(11), 2014-2037 (2017)
51. Maeder, M., King, P.: Analysis of Chemical Processes, Determination of the Reaction Mechanism and Fitting of Equilibrium and/or Rate Constants. (2012)
52. Leggett, D.J., Kelly, S.L., Shiue, L.R., Wu, Y.T., Chang, D., Kadish, K.M.: A computational approach to the spectrophotometric determination of stability constants-II. Application to metalloporphyrin-axial ligand interactions in non-aqueous solvents. Talanta **30**(8), 579-586 (1983)
53. Ribeiro, A.R., Schmidt, T.C.: Determination of acid dissociation constants (pK(a)) of. cephalosporin antibiotics: Computational and experimental approaches. Chemosphere **169**, 524-533 (2017)
54. ACD/Labs pKa Predictor 3.0. In: Inc., A.C.D. (ed.). Toronto, Canada, (2007)
55. Balogh, G.T., Gyarmati, B., Nagy, B., Molnar, L., Keseru, G.M.: Comparative Evaluation of in Silico pK(a) Prediction Tools on the Gold Standard Dataset. Qsar Comb Sci **28**(10), 1148-1155 (2009)
56. Balogh, G.T., Tarcsay, A., Keseru, G.M.: Comparative evaluation of pK(a) prediction tools on a drug discovery dataset. Journal of Pharmaceutical and Biomedical Analysis **67-68**, 63-70 (2012)
57. Evagelou, V., Tsantili-Kakoulidou, A., Koupparis, M.: Determination of the dissociation constants of the cephalosporins cefepime and cefpirome using UV spectrometry and pH potentiometry. Journal of Pharmaceutical and Biomedical Analysis **31**(6), 1119-1128 (2003)
58. Liao, C.Z., Nicklaus, M.C.: Comparison of Nine Programs Predicting pK(a) Values of Pharmaceutical Substances. J Chem Inf Model **49**(12), 2801-2812 (2009)
59. Roda, G., Dallanoce, C., Grazioso, G., Liberti, V., De Amici, M.: Determination of Acid Dissociation Constants of Compounds Active at Neuronal Nicotinic Acetylcholine Receptors by Means of Electrophoretic and Potentiometric Techniques. Anal Sci **26**(1), 51-54 (2010)
60. Bezencon, J., Wittwer, M.B., Cutting, B., Smiesko, M., Wagner, B., Kansy, M., Ernst, B.: pK(a) determination by H-1 NMR spectroscopy - An old methodology revisited. Journal of Pharmaceutical and Biomedical Analysis **93**, 147-155 (2014)
61. Hansen, N.T., Kouskoumvekaki, I., Jorgensen, F.S., Brunak, S., Jonsdottir, S.O.: Prediction of pH-dependent aqueous solubility of druglike molecules. J Chem Inf Model **46**(6), 2601-2609 (2006)
62. Manchester, J., Walkup, G., Rivin, O., You, Z.P.: Evaluation of pK(a) Estimation Methods on 211 Drug like Compounds. J Chem Inf Model **50**(4), 565-571 (2010)
63. ten Brink, T., Exner, T.E.: pK(a) based protonation states and microspecies for protein-ligand docking. J Comput Aid Mol Des **24**(11), 935-942 (2010)
64. Terminology, I.C.o.C.: IUPAC Gold Book (International Union of Pure and Applied Chemistry), vol. Version 2.3.3 (2014-02-24), Version 2.3.3 ed., (2014)
65. Meloun, M., Syrový, T., Bordovská, S., Vrána, A.: Reliability and uncertainty in the estimation of pK (a) by least squares nonlinear regression analysis of multiwavelength spectrophotometric pH titration data. Anal Bioanal Chem **387**(3), 941-955 (2007)
66. Meloun, M., Havel, J., Högfeldt, E.: Computation of solution equilibria: A guide to methods in potentiometry, extraction, and spectrophotometry. Ellis Horwood series in analytical chemistry. Ellis Horwood Chichester, England (1988)

67. Rigano, C., Grasso, M., Sammartano, S.: Computer-Analysis of Equilibrium Data in Solution - a Compact Least-Squares Computer-Program for Acid-Base Titrations. Annali Di Chimica **74**(7-8), 537-532 (1984)
68. Meloun, M., Čapek, J., Mikšík, P., Brereton, R.G.: Critical comparison of methods predicting the number of components in spectroscopic data. Anal Chim Acta **423**(1), 51-68 (2000)
69. ORIGIN. In. OriginLab Corporation, One Roundhouse Plaza, Suite 303, Northampton, MA 01060, USA.,
70. Ramos, J.A.M.: UV-VIS Spectrometry, pKa of a dye. (2014)
71. Albert, A., Goldacre, R., Phillips, J.,: The Strength of heterocyclic bases. Journal of Chemical Society 2240-2249 (1948)
72. Meloun, M., Militký, J., Forina, M.: Chemometrics for analytical chemistry, Volume 2: PC- aided regression and related methods. Chemometrics for analytical chemistry. Ellis Horwood, Chichester (1994)
73. Meloun, M., Militký, J., Forina, M.: Chemometrics for analytical chemistry, Volume 1: PC-Aided Statistical Data Analysis. Chemometrics for analytical chemistry. Ellis Horwood, Chichester (1992)

Figure captions

Fig. 1 The structural formula of Roxadustat.

Fig. 2 (a) The 3D-absorbance response surface on pH for Roxadustat, (b) Predicted species of the protonated equilibria contained 1 cation, 3 anions, 1 ampholyte and 1 neutral molecule. (c) The molecular structure of Roxadustat (inset) with highlighted basic centres A, B, C, D, E and F and predicted pK_a values using MARVIN/ACD prediction programs. The structure of auxiliary fragments 1-3 and their predicted pK_a. (d) The distribution diagram of the relative contractions [%] of variously protonated species of Roxadustat are related to the predicted dissociation constants.

Fig. 3 (a) The entire spectrum of Roxadustat was divided into the three following subspectra (b), (c) and (d). By changing the solution pH, the absorbance of the chromophore was changed, and this change has to be examined in three pH ranges: (b) Small changes of the absorbance marked Delta A (the right axes on (b)) were detected in estimation of the pK_1 in the pH range 2.6 - 4.2, as well as (c) the estimation of the pK_2 and pK_3 in the pH range 4.2 - 8.1. (d) Sufficiently large changes of the absorbance occurred only in estimation of the pK_4 in the range of 8.2 - 11.6. (e) The modification of the Cattel's scree plot log $s_k(SV) = f(k)$ of the of singular value decomposition SVD served to the rank estimation of the absorbance matrix. The residual standard deviation RSD lead to $k^* = 5$ and (f) in the logarithmic scale is lead to $k^* = 5$ which means that it was valid that $n_c = 5$, (INDICES in S-PLUS), [42].

Fig. 4 A typical SQUAD84 working environment searching for the best protonation model of Roxadustat in the pH range from 2,5 to 11,6 for a model of two, three and four dissociation constants pK_{a1}, pK_{a2}, pK_{a3}, pK_{a4} at $I = 0.0026$ and 25°C. *Left:* The pure spectra profiles of molar absorptivity *vs*. wavelength (nm) for all of the

variously protonated species of Roxadustat. *Right:* The distribution diagram of the relative concentrations of all of the variously protonated species in dependence on pH, (REACTLAB, ORIGIN 9).

Fig. 5 (a) The entire spectrum of Roxadustat in 220 – 410 nm is distinguished into five absorption bands with five isosbestic points. The isosbestic points regarded the protonation equilibrium LH^{2-}/L^{3-}, while the spectra of the other protonation equlibria disturb the position of the intersection at the isosbestic point for LH^{2-}/L^{3-}. (b) The positions of the isosbestic points are also shown in the graph of the molar absorption coefficients vs. wavelength for variously protonated Roxadustat.

Fig. 6 The experimental strategy of the optioned wavelengths range concerns the dependence of the proximity between the ionisable group and the chromophore as the spectral shift might not be strong enough to allow a successful determination of a model of dissociation constants. The model of 3 pK_a (left column) and 4 pK_a (right column) estimated from the entire spectrum of wavelength A - D is compared with those estimated from three separate absorption bands, 220 – 270 nm, 260 – 320 nm, and 320 – 410 nm. The best spectra fitness $s(A)$ is in the wavelength range 260 – 320 nm, although the pK_a estimates were nearly the same in all three ranges. Here n means the number of pH and m is the number of wavelengths of every spectrum.

Fig. 7 The change of pH did not cause the same changes in the Roxadustat spectrum because some chromophores are only slightly affected by a pH change. (a) The spectra of molar absorption coefficients on wavelength contains positions of six wavelengths, A through F, at which the following A-pH curves were analysed. (b) The distribution diagram of the relative concentration of all variously protonated species also indicated consecutive equilibria with the close dissociation constants. The A-pH graphs A through F demonstrate a sensitivity of chromophores in Roxadustat molecule on pH changes. The maximum absorbance shifts at pH changes in range of 2.6 – 11.6 estimating pK_1 were 100 (at position A), 140 (at B), 60 (at C), 40 (at D), 50 (at E) and 60 mAU (at F), which lead to the mean 75.0 mAU. Analogically, for an estimation of pK_2 they were 130, 100, 70, 40, 50 and 50 with the mean 73.3 mAU. For the estimation pK_3 they were 50, 120, 150, 50, 30 and 80 with the mean 80.0 mAU, and finally the largest shifts of absorbance to estimate pK_4 were 350, 240, 260, 130, 90 and 300 with the mean 228.3 mAU.

Fig. 8 The reproducibility of the dissociation constants of Roxadustat estimated from five reproduced measurements (UV-metric, graph a and c) and seven reproduced measurements (pH-metric, graph b and d) were found to be in good agreement at 25°C (Table 1). The reproducibility of the protonation model estimates with three (a, c) and four (b, d) dissociation constants are compared. The arithmetic mean of the dissociation constants with their standard deviation and spectra-fitness was expressed as the standard deviation $s(A)$ and $s(V)$. Both instrumental methods found better curve-fitness achieved with the model of four dissociation constants (REACTLAB, SQUAD84, ORIGIN 9).

Fig. 9 (a) The 2D-plot of absorbance changes in the Roxadustat 2D-spectra set were within pH-titration. (b) The set of A-pH curves at selected wavelength shows a sensitivity of chromophores in Roxadustat on the pH change. (c) The plot of the absorbance shift Δ_{ij} in the Roxadustat spectrum within pH-titration when the value of the absorbance difference for the jth-wavelength of the ith-spectrum is expressed $\Delta_{ij} = A_{ij} - A_{i,\mathrm{acid}}$. This absorbance changes Δ were plotted on wavelength λ. Here $A_{i,\mathrm{acid}}$ stood for the limiting spectrum of the acid form of the Roxadustat. (d) Residuals ***e*** [mAU] were tested if they were of the same magnitude as the instrumental noise $s_{\mathrm{inst}}(A)$, (REACTLAB, ORIGIN 9).

Fig. 10 Deconvolution of the each experimental spectrum (exp) of 8.0×10^{-5} mol. dm^{-3} Roxadustat at I = 0.0081 at 25°C into spectra of the the individual variously protonated species L^{3-}, LH^{2-}, LH_2^-, LH_3, LH_4^+ in mixture for pH 2.92, 3.40, 4.04, 5.47, 6.28, 8.09, 9.02 and 9.77 using SQUAD84.

Fig. 11 The search for the protonation model with the potentiometric pH-metric method for 3 (Fig. 11a and 11c) and 4 dissociation constants (Fig. 11b and 11d). The pH-titration curve of alkalized Roxadustat is titrated with HCl and plotted with the Bjerrum protonation function comparing 3 and 4 pK_a. Dissociation constants were estimated with ESAB at 25°C (ESAB, ORIGIN).

Fig. 12 The extrapolation of the mixed dissociation constants of Roxadustat on the square root of the ionic strength for four dissociation constants leading to the thermodynamic dissociation constant pK^T_a at 25°C (*Left*) and 37°C (*Right*) using UV-metric technique (*Upper*) and pH-metric (*Lower*). The Working-Hotelling confidence bands express the uncertainty of the each dissociation constant estimate, since the broader band is the more uncertain pK_a.

Scheme 1 The protonation scheme of Roxadustat.

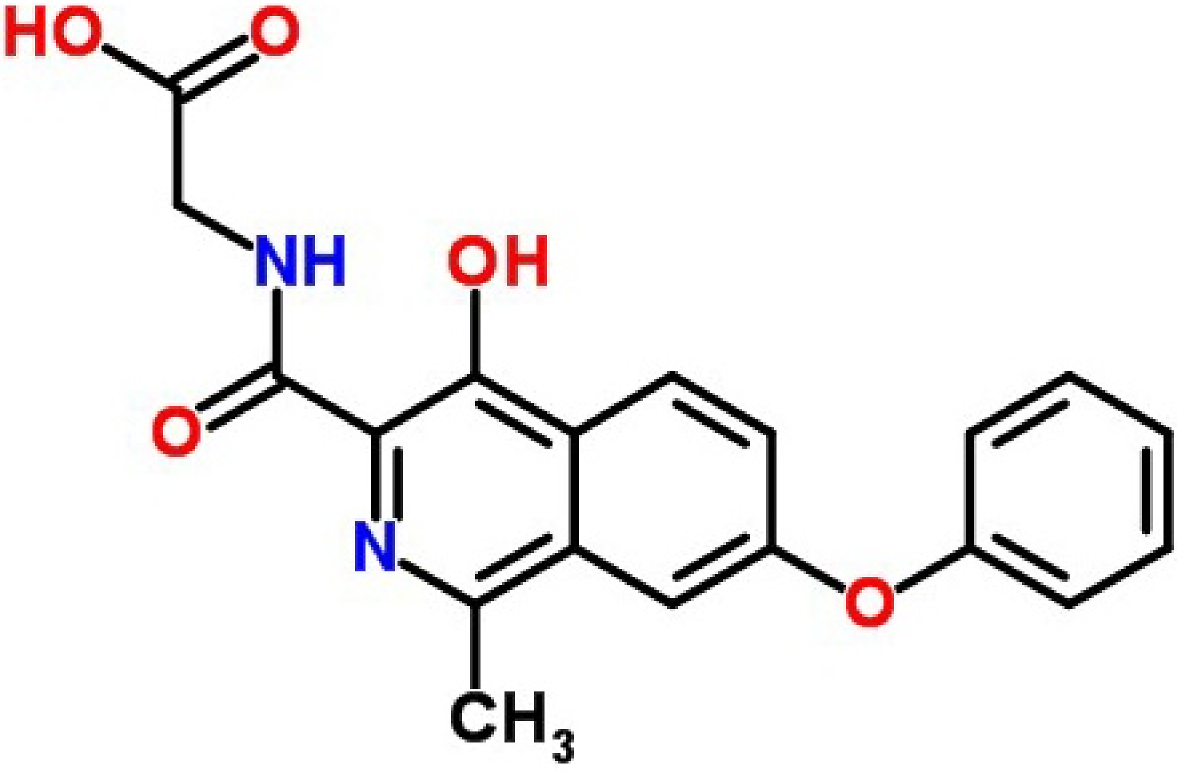

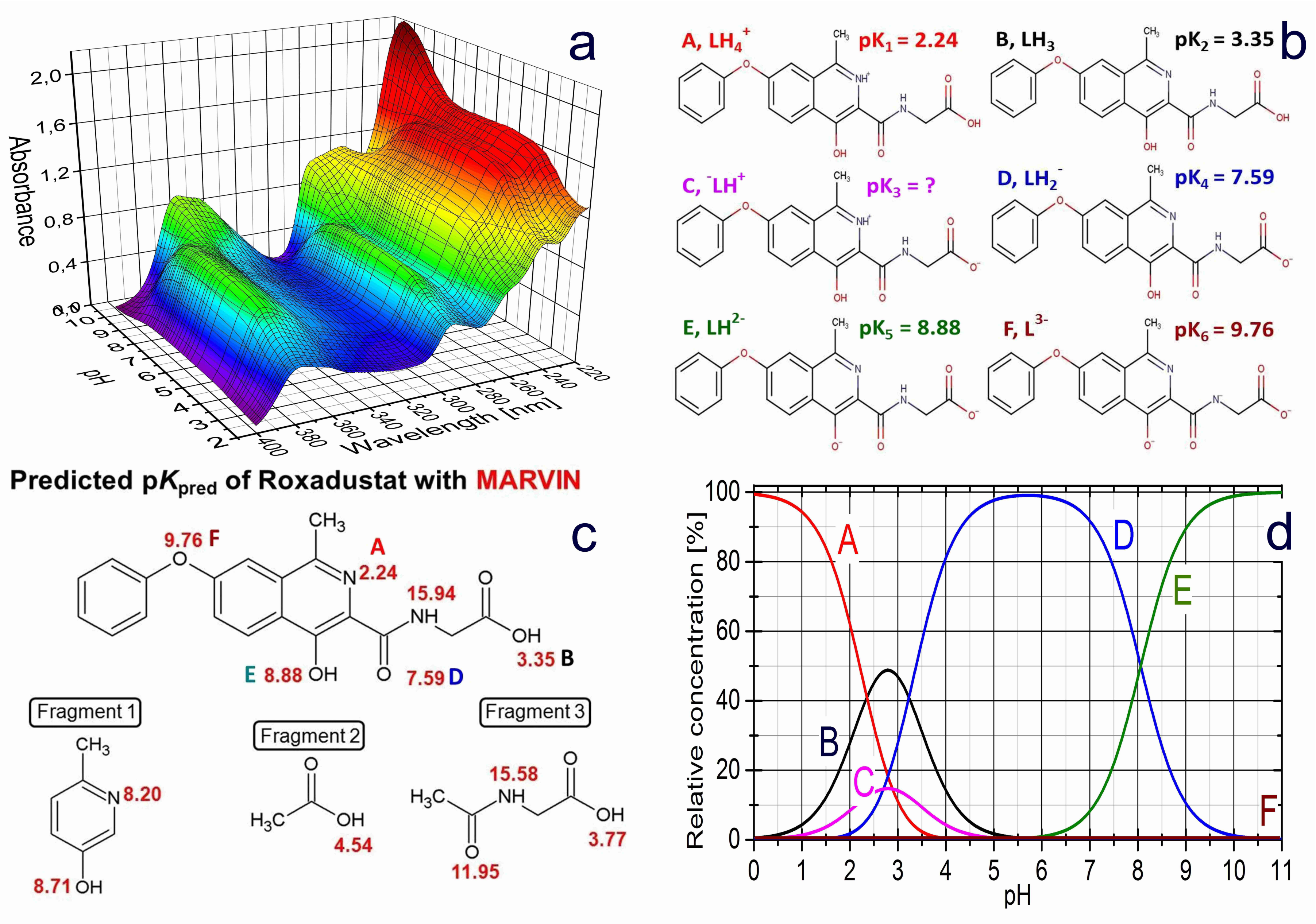
a
Absorbance
2,0
1,6
1,2
0,8
0,4
0,0
pH
10
9
8
7
6
5
4
3
2
Wavelength [nm]
400
380
360
340
320
300
280
260
240
220
b
A, LH_4^+
$pK_1 = 2.24$
B, LH_3
$pK_2 = 3.35$
C, $^-LH^+$
$pK_3 = ?$
D, LH_2^-
$pK_4 = 7.59$
E, LH^{2-}
$pK_5 = 8.88$
F, L^{3-}
$pK_6 = 9.76$
CH_3
NH^+
N
H
O
OH
O^-
N^-
Predicted pK_{pred} of Roxadustat with MARVIN
c
CH_3
9.76 F
A
N 2.24
15.94
NH
O
OH
3.35 B
E 8.88 OH
O
7.59 D
Fragment 1
CH_3
N 8.20
8.71 OH
Fragment 2
H_3C
O
OH
4.54
Fragment 3
15.58
H_3C
NH
O
OH
11.95
3.77
d
Relative concentration [%]
100
80
60
40
20
0
pH
0
1
2
3
4
5
6
7
8
9
10
11
A
B
C
D
E
F

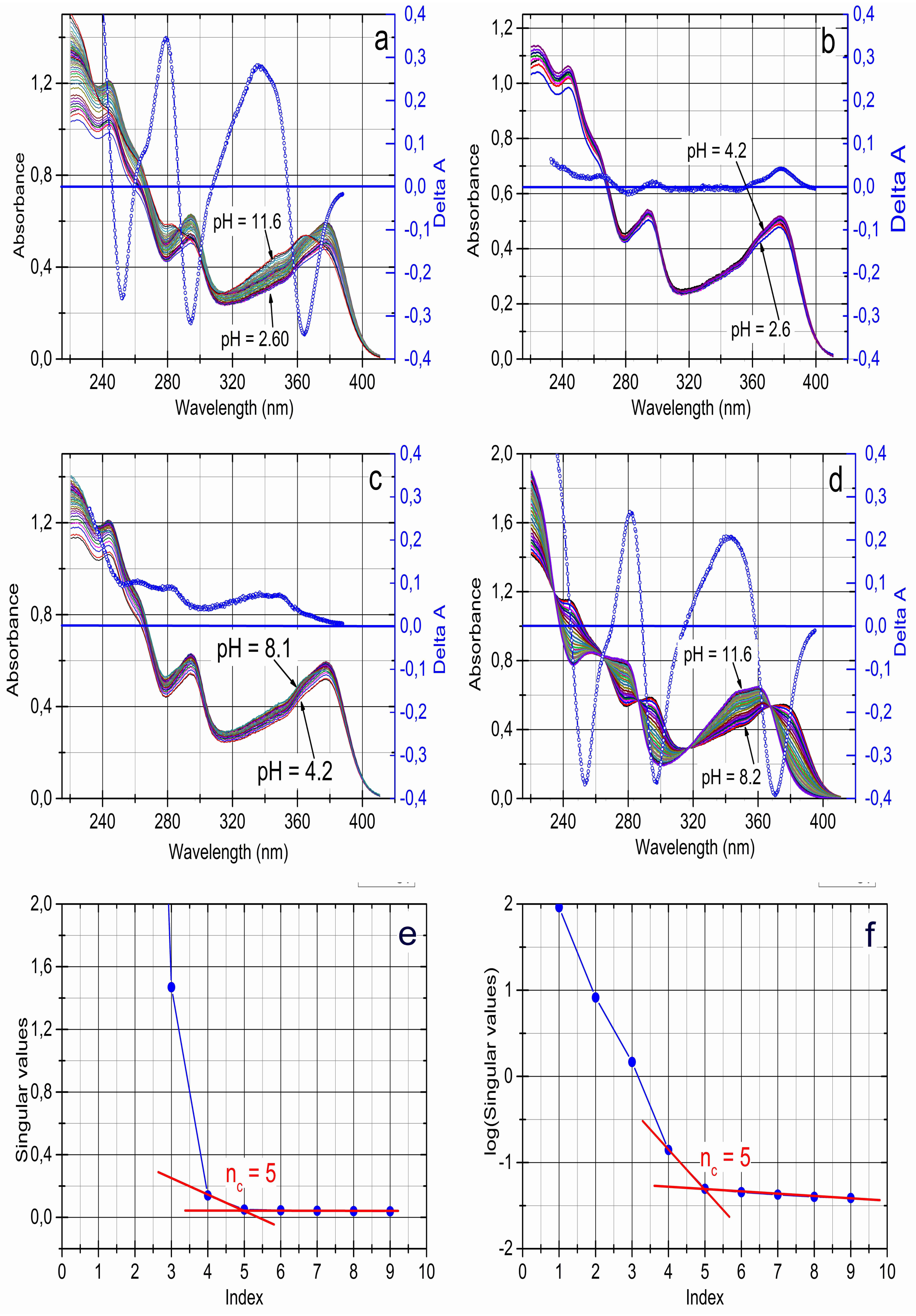
a
Absorbance
Delta A
Wavelength (nm)
pH = 11.6
pH = 2.60
b
pH = 4.2
pH = 2.6
c
pH = 8.1
pH = 4.2
d
pH = 11.6
pH = 8.2
e
Singular values
Index
$n_c = 5$
f
log(Singular values)
Index
$n_c = 5$

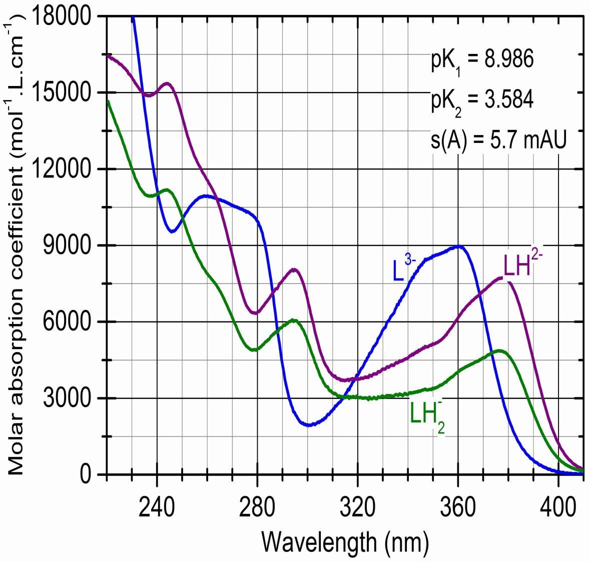
Molar absorption coefficient (mol^{-1}.L.cm^{-1})
18000
15000
12000
9000
6000
3000
0
240
280
320
360
400
Wavelength (nm)
pK$_1$ = 8.986
pK$_2$ = 3.584
s(A) = 5.7 mAU
L^{3-}
LH^{2-}
LH$_2^-$

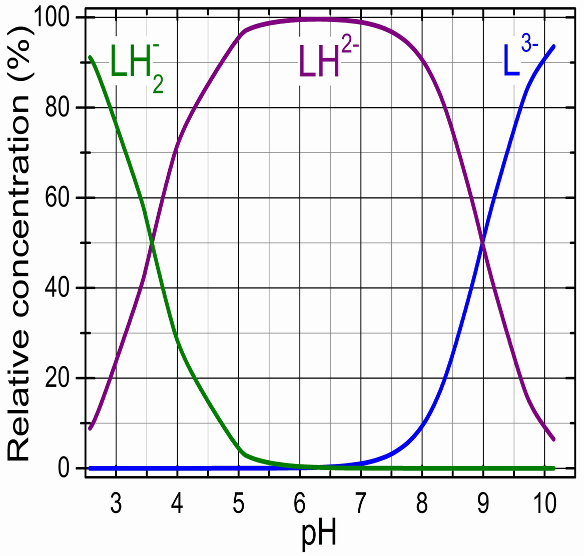
Relative concentration (%)
100
80
60
40
20
0
3
4
5
6
7
8
9
10
pH
LH$_2^-$
LH^{2-}
L^{3-}

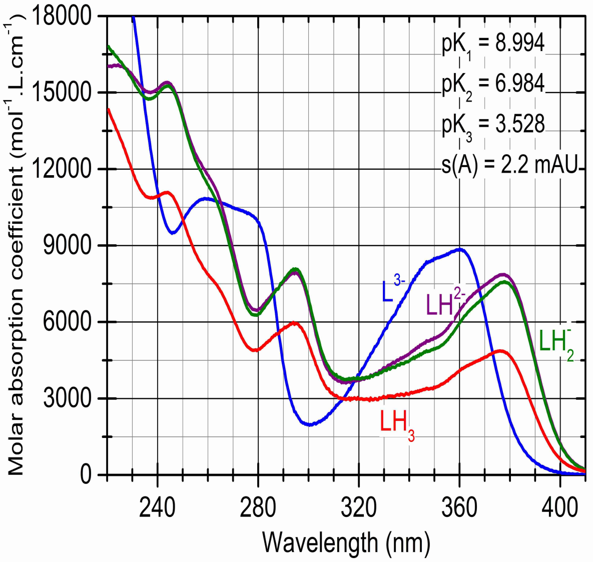
Molar absorption coefficient (mol^{-1}.L.cm^{-1})
18000
15000
12000
9000
6000
3000
0
240
280
320
360
400
Wavelength (nm)
pK$_1$ = 8.994
pK$_2$ = 6.984
pK$_3$ = 3.528
s(A) = 2.2 mAU
L^{3-}
LH^{2-}
LH$_2^-$
LH$_3$

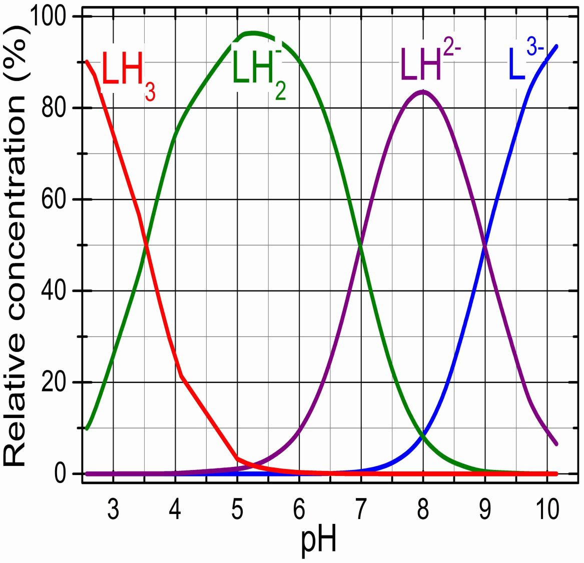
Relative concentration (%)
100
80
60
40
20
0
3
4
5
6
7
8
9
10
pH
LH$_3$
LH$_2^-$
LH^{2-}
L^{3-}

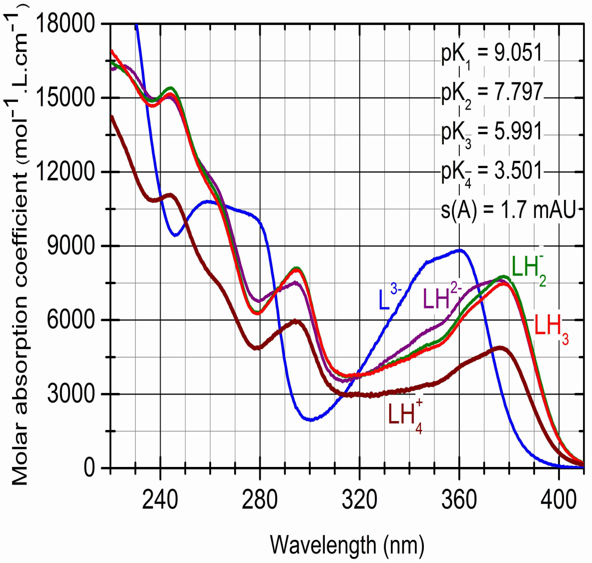
Molar absorption coefficient (mol^{-1}.L.cm^{-1})
18000
15000
12000
9000
6000
3000
0
240
280
320
360
400
Wavelength (nm)
pK$_1$ = 9.051
pK$_2$ = 7.797
pK$_3$ = 5.991
pK$_4$ = 3.501
s(A) = 1.7 mAU
L^{3-}
LH^{2-}
LH$_2^-$
LH$_3$
LH$_4^+$

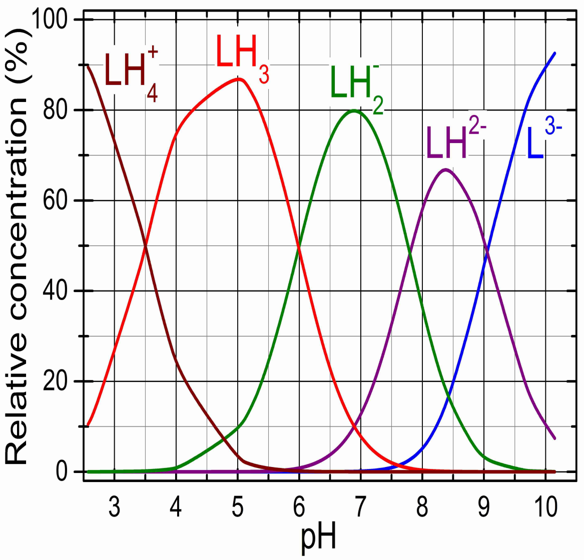
Relative concentration (%)
100
80
60
40
20
0
3
4
5
6
7
8
9
10
pH
LH$_4^+$
LH$_3$
LH$_2^-$
LH^{2-}
L^{3-}

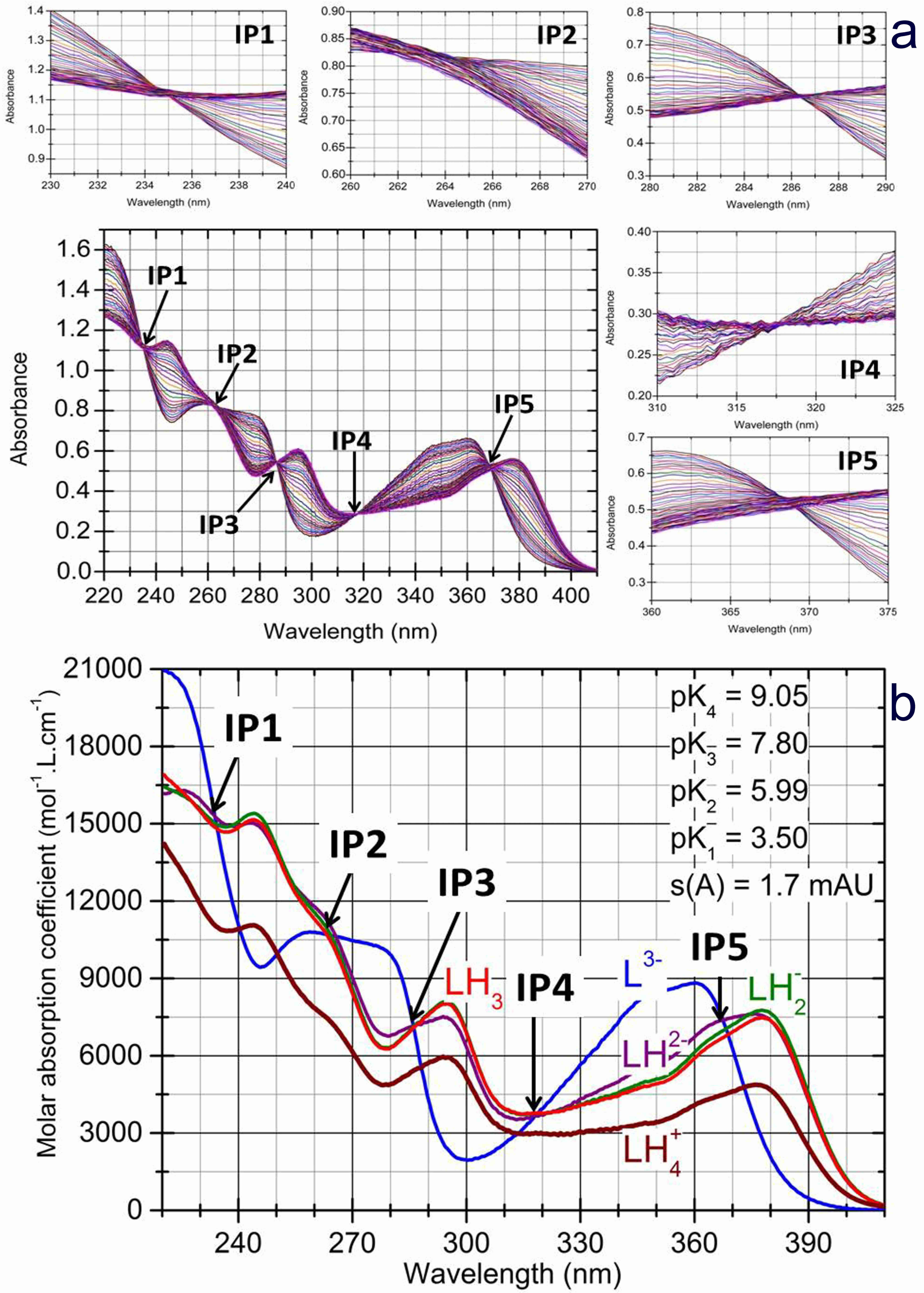
a
IP1
Absorbance
Wavelength (nm)
IP2
IP3
IP4
IP5
Absorbance
Wavelength (nm)
b
pK$_4$ = 9.05
pK$_3$ = 7.80
pK$_2$ = 5.99
pK$_1$ = 3.50
s(A) = 1.7 mAU
IP1
IP2
IP3
IP4
IP5
LH$_3$
L^{3-}
LH$_2^-$
LH^{2-}
LH$_4^+$
Molar absorption coefficient (mol^{-1}.L.cm^{-1})
Wavelength (nm)

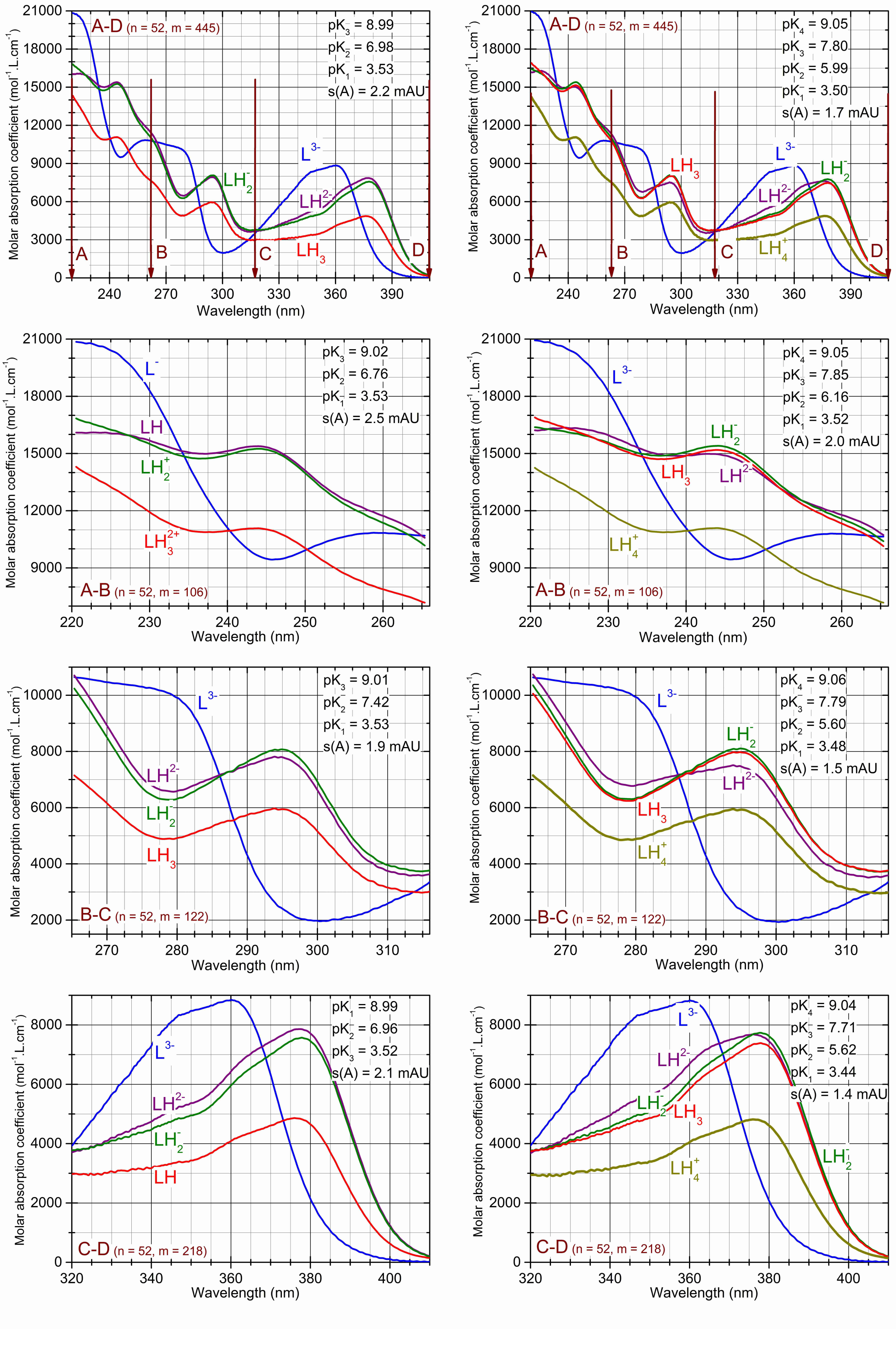
A-D (n = 52, m = 445)
pK$_3$ = 8.99
pK$_2$ = 6.98
pK$_1$ = 3.53
s(A) = 2.2 mAU
A
B
C
D
L^{3-}
LH$_2^-$
LH^{2-}
LH$_3$
A-D (n = 52, m = 445)
pK$_4$ = 9.05
pK$_3$ = 7.80
pK$_2$ = 5.99
pK$_1$ = 3.50
s(A) = 1.7 mAU
A
B
C
D
L^{3-}
LH$_3$
LH^{2-}
LH$_2^-$
LH$_4^+$
A-B (n = 52, m = 106)
pK$_3$ = 9.02
pK$_2$ = 6.76
pK$_1$ = 3.53
s(A) = 2.5 mAU
L$^-$
LH
LH$_2^+$
LH$_3^{2+}$
A-B (n = 52, m = 106)
pK$_4$ = 9.05
pK$_3$ = 7.85
pK$_2$ = 6.16
pK$_1$ = 3.52
s(A) = 2.0 mAU
L^{3-}
LH$_2^-$
LH$_3$
LH^{2-}
LH$_4^+$
B-C (n = 52, m = 122)
pK$_3$ = 9.01
pK$_2$ = 7.42
pK$_1$ = 3.53
s(A) = 1.9 mAU
L^{3-}
LH^{2-}
LH$_2^-$
LH$_3$
B-C (n = 52, m = 122)
pK$_4$ = 9.06
pK$_3$ = 7.79
pK$_2$ = 5.60
pK$_1$ = 3.48
s(A) = 1.5 mAU
L^{3-}
LH$_2^-$
LH^{2-}
LH$_3$
LH$_4^+$
C-D (n = 52, m = 218)
pK$_1$ = 8.99
pK$_2$ = 6.96
pK$_3$ = 3.52
s(A) = 2.1 mAU
L^{3-}
LH^{2-}
LH$_2^-$
LH
C-D (n = 52, m = 218)
pK$_4$ = 9.04
pK$_3$ = 7.71
pK$_2$ = 5.62
pK$_1$ = 3.44
s(A) = 1.4 mAU
L^{3-}
LH^{2-}
LH$_2^-$
LH$_3$
LH$_4^+$
LH$_2^-$
Molar absorption coefficient (mol^{-1}.L.cm^{-1})
Wavelength (nm)

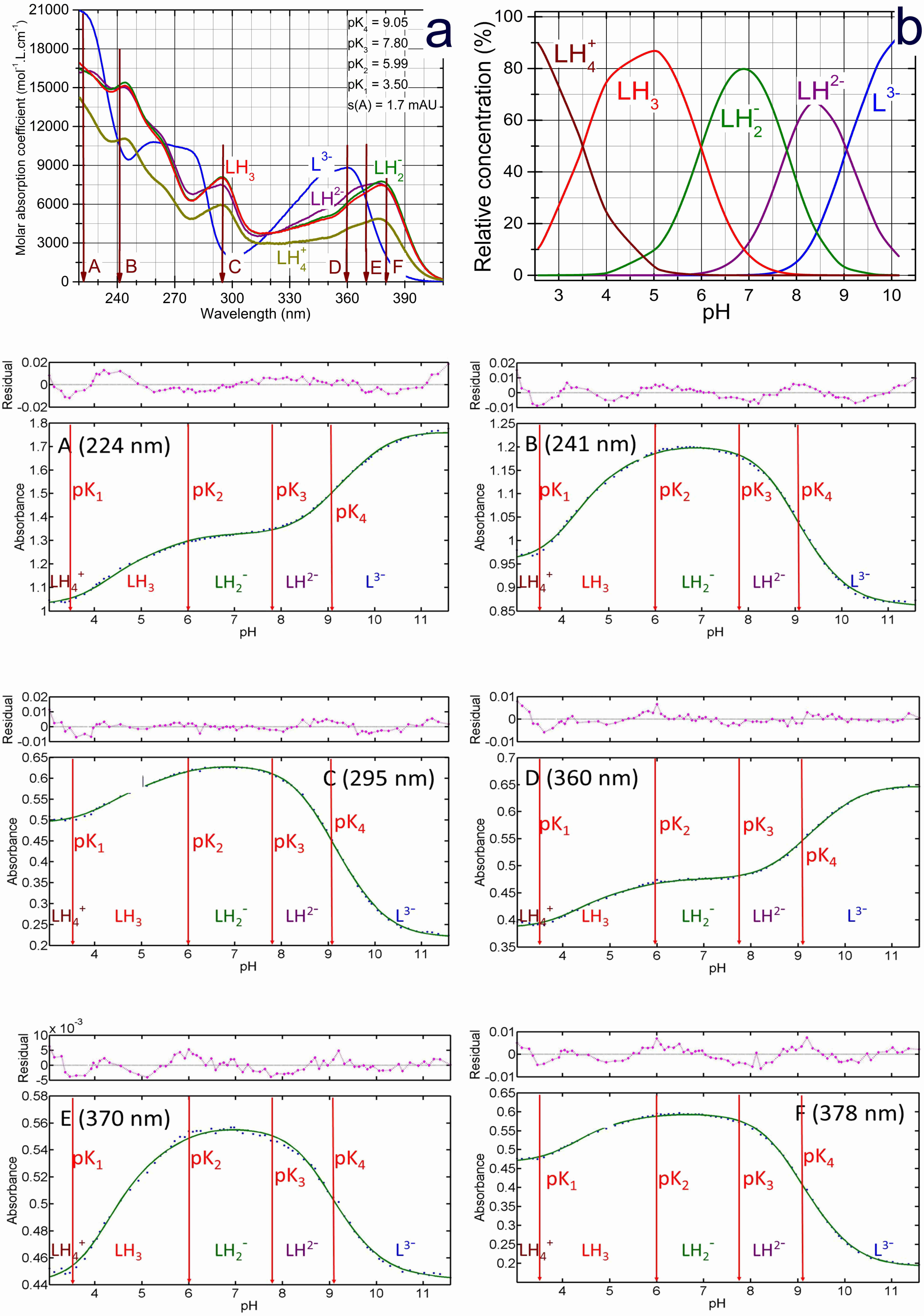
a
pK4 = 9.05
pK3 = 7.80
pK2 = 5.99
pK1 = 3.50
s(A) = 1.7 mAU
Molar absorption coefficient (mol-1.L.cm-1)
Wavelength (nm)
LH3
L3-
LH2-
LH2-
LH4+
A
B
C
D
E
F
b
Relative concentration (%)
pH
LH4+
LH3
LH2-
LH2-
L3-
A (224 nm)
B (241 nm)
C (295 nm)
D (360 nm)
E (370 nm)
F (378 nm)
Residual
Absorbance
pH
pK1
pK2
pK3
pK4
LH4+
LH3
LH2-
LH2-
L3-
x 10-3

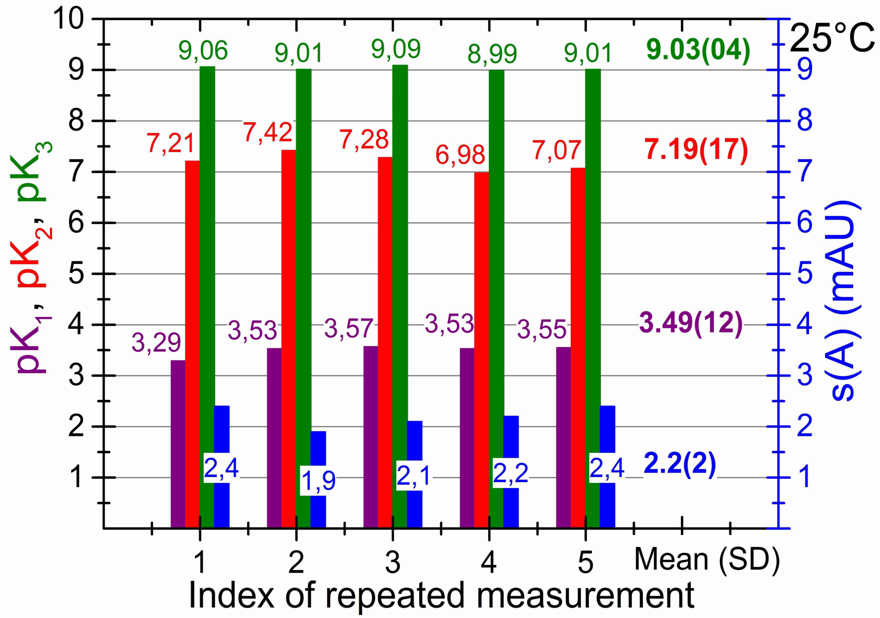
25°C
pK_1, pK_2, pK_3
s(A) (mAU)
Index of repeated measurement
1
2
3
4
5
Mean (SD)
9,06
9,01
9,09
8,99
9,01
9.03(04)
7,21
7,42
7,28
6,98
7,07
7.19(17)
3,29
3,53
3,57
3,53
3,55
3.49(12)
2,4
1,9
2,1
2,2
2,4
2.2(2)
10
9
8
7
6
5
4
3
2
1

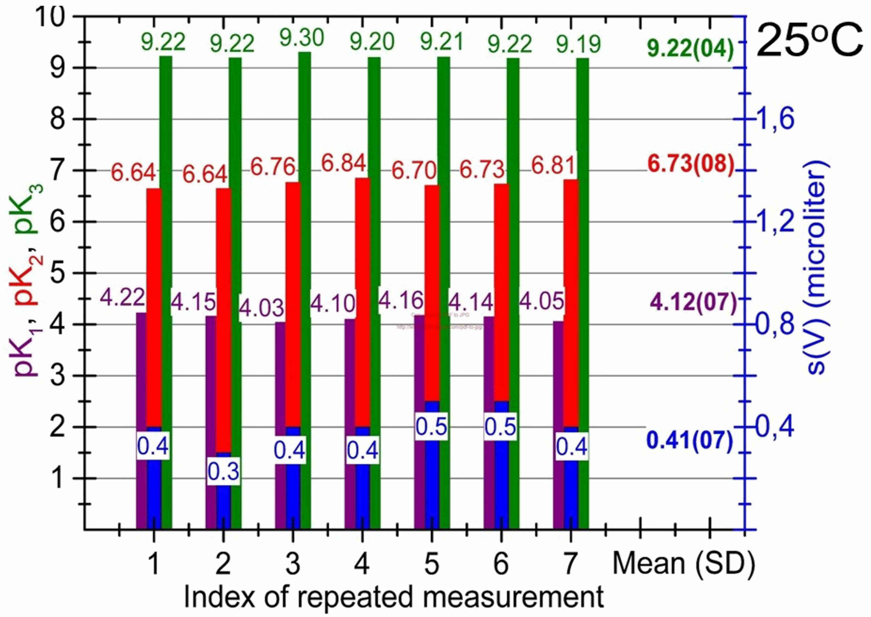
25°C
pK_1, pK_2, pK_3
s(V) (microliter)
Index of repeated measurement
1
2
3
4
5
6
7
Mean (SD)
9.22
9.22
9.30
9.20
9.21
9.22
9.19
9.22(04)
6.64
6.64
6.76
6.84
6.70
6.73
6.81
6.73(08)
4.22
4.15
4.03
4.10
4.16
4.14
4.05
4.12(07)
0.4
0.3
0.4
0.4
0.5
0.5
0.4
0.41(07)
10
9
8
7
6
5
4
3
2
1
1,6
1,2
0,8
0,4

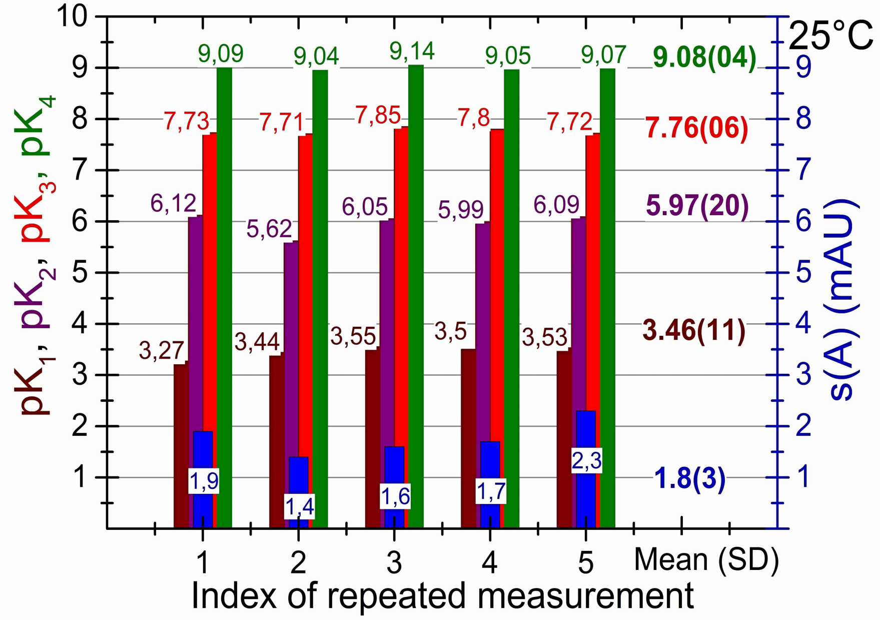
25°C
pK_1, pK_2, pK_3, pK_4
s(A) (mAU)
Index of repeated measurement
1
2
3
4
5
Mean (SD)
9,09
9,04
9,14
9,05
9,07
9.08(04)
7,73
7,71
7,85
7,8
7,72
7.76(06)
6,12
5,62
6,05
5,99
6,09
5.97(20)
3,27
3,44
3,55
3,5
3,53
3.46(11)
1,9
1,4
1,6
1,7
2,3
1.8(3)
10
9
8
7
6
5
4
3
2
1

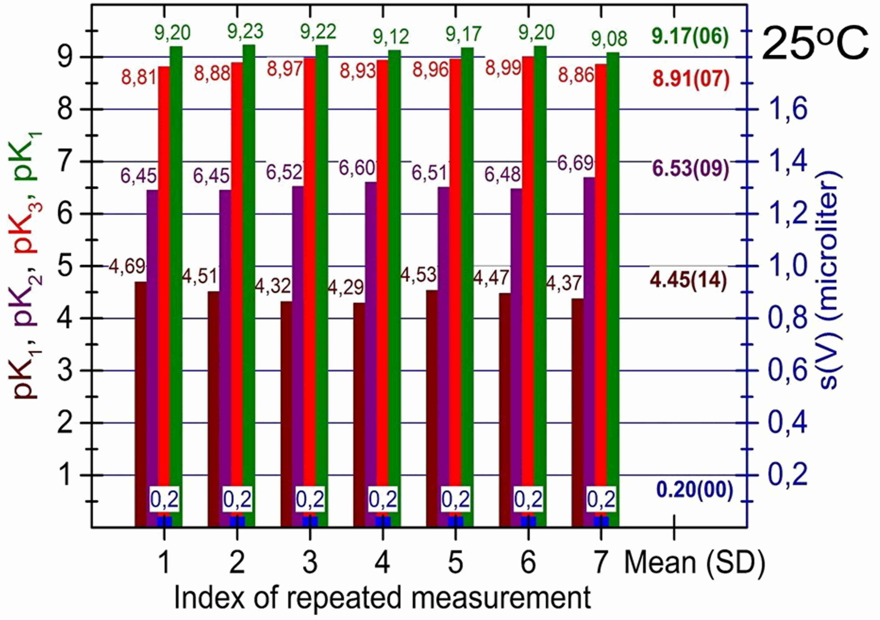
25°C
pK_1, pK_2, pK_3, pK_1
s(V) (microliter)
Index of repeated measurement
1
2
3
4
5
6
7
Mean (SD)
9,20
9,23
9,22
9,12
9,17
9,20
9,08
9.17(06)
8,81
8,88
8,97
8,93
8,96
8,99
8,86
8.91(07)
6,45
6,45
6,52
6,60
6,51
6,48
6,69
6.53(09)
4,69
4,51
4,32
4,29
4,53
4,47
4,37
4.45(14)
0,2
0,2
0,2
0,2
0,2
0,2
0,2
0.20(00)
9
8
7
6
5
4
3
2
1
1,6
1,4
1,2
1,0
0,8
0,6
0,4
0,2

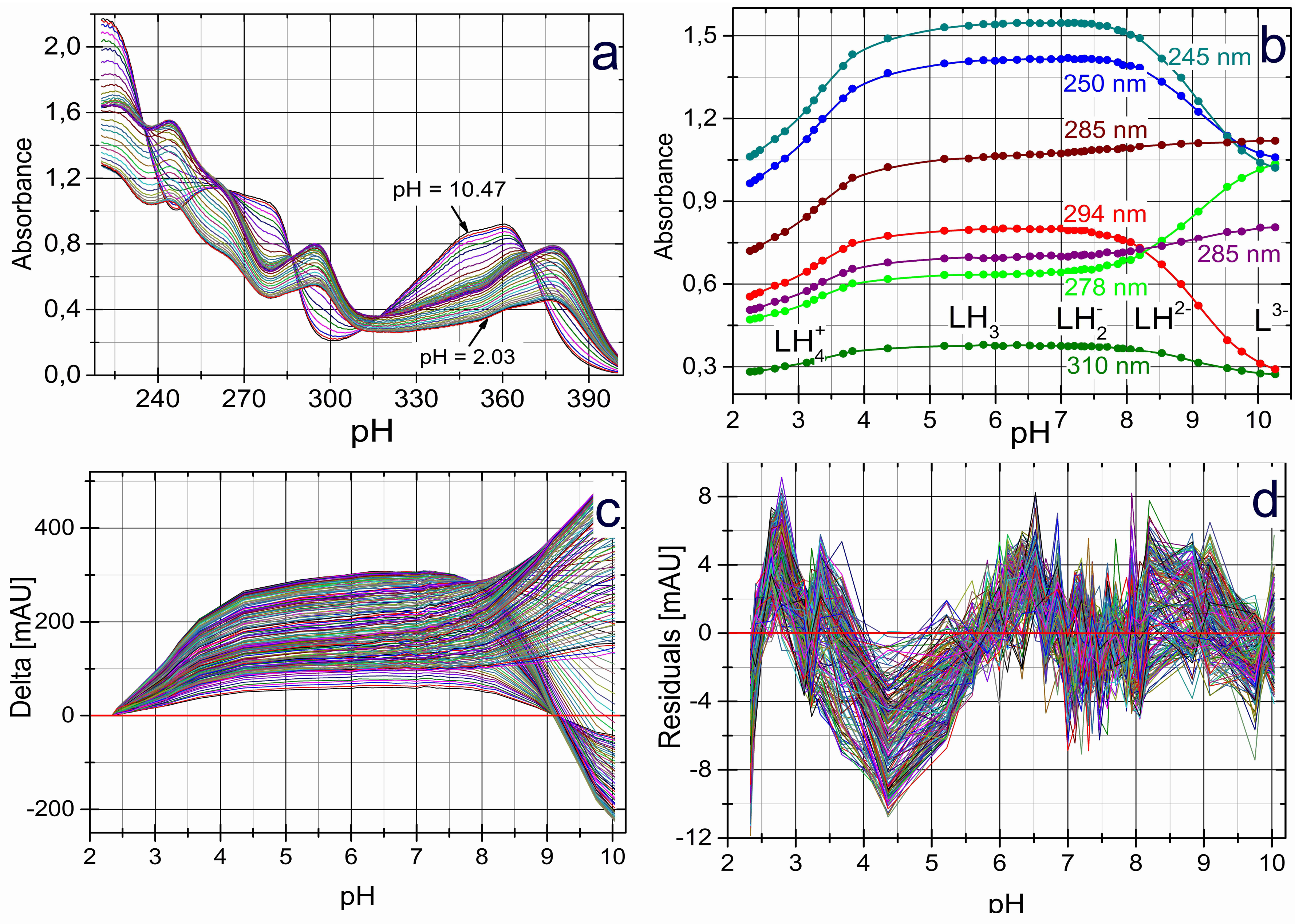
a
Absorbance
2,0
1,6
1,2
0,8
0,4
0,0
240
270
300
330
360
390
pH
pH = 10.47
pH = 2.03
b
Absorbance
1,5
1,2
0,9
0,6
0,3
245 nm
250 nm
285 nm
294 nm
285 nm
278 nm
310 nm
LH_4^+
LH_3
LH_2^-
LH^{2-}
L^{3-}
2
3
4
5
6
7
8
9
10
pH
c
Delta [mAU]
400
200
0
-200
2
3
4
5
6
7
8
9
10
pH
d
Residuals [mAU]
8
4
0
-4
-8
-12
2
3
4
5
6
7
8
9
10
pH

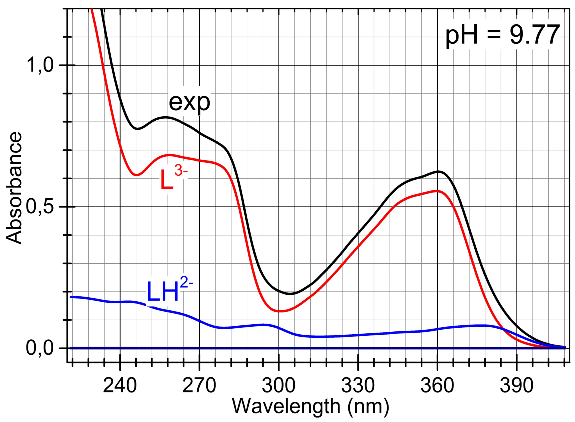
pH = 9.77
exp
L^{3-}
LH^{2-}
Absorbance
0,0
0,5
1,0
240
270
300
330
360
390
Wavelength (nm)

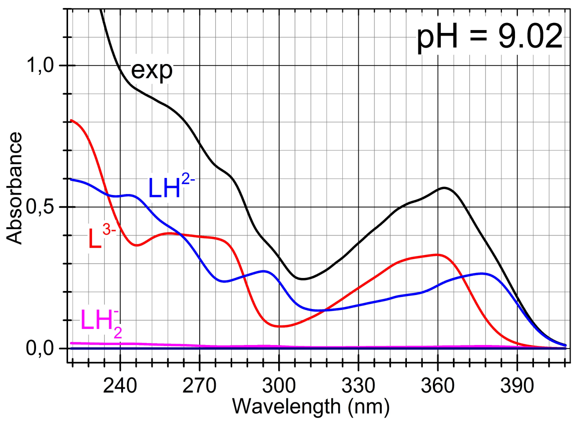
pH = 9.02
exp
LH^{2-}
L^{3-}
LH_2^-
Absorbance
0,0
0,5
1,0
240
270
300
330
360
390
Wavelength (nm)

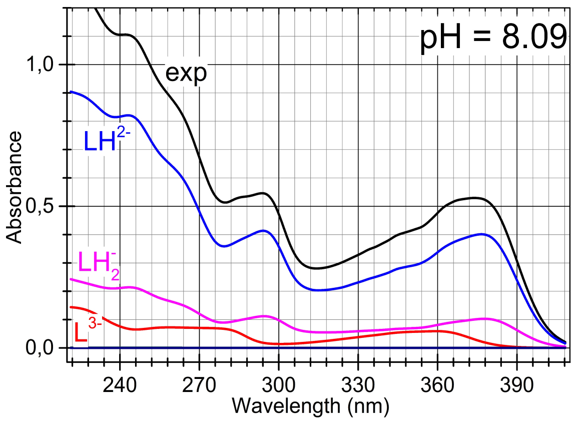
pH = 8.09
exp
LH^{2-}
LH_2^-
L^{3-}
Absorbance
0,0
0,5
1,0
240
270
300
330
360
390
Wavelength (nm)

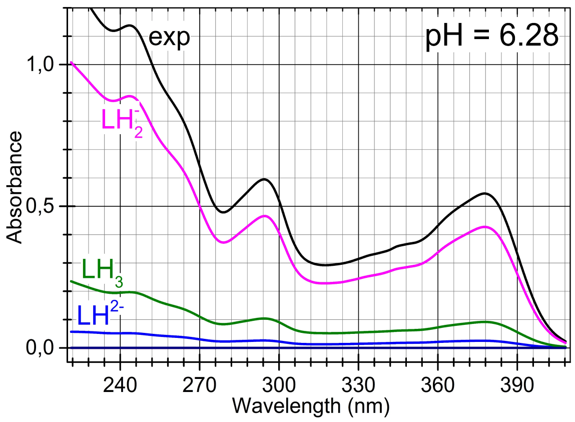
pH = 6.28
exp
LH_2^-
LH_3
LH^{2-}
Absorbance
0,0
0,5
1,0
240
270
300
330
360
390
Wavelength (nm)

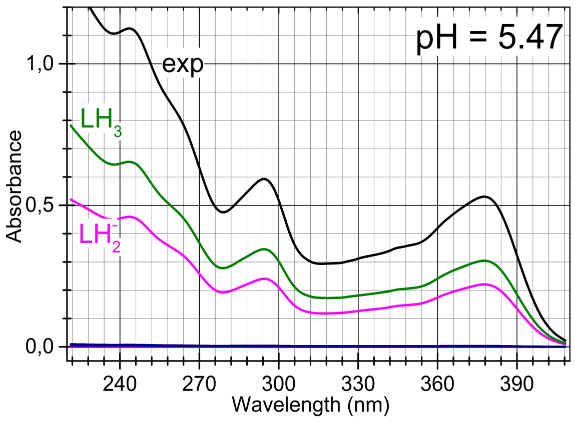
pH = 5.47
exp
LH_3
LH_2^-
Absorbance
0,0
0,5
1,0
240
270
300
330
360
390
Wavelength (nm)

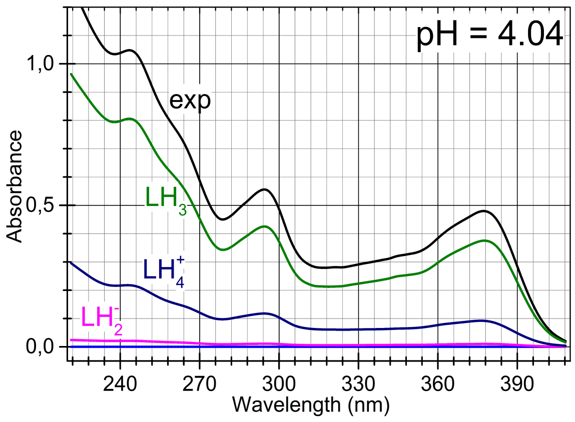
pH = 4.04
exp
LH_3
LH_4^+
LH_2^-
Absorbance
0,0
0,5
1,0
240
270
300
330
360
390
Wavelength (nm)

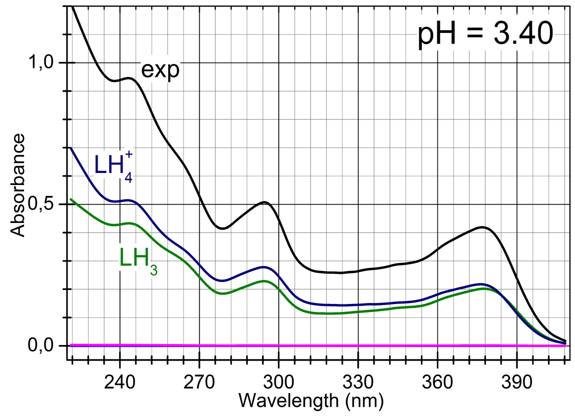
pH = 3.40
exp
LH_4^+
LH_3
Absorbance
0,0
0,5
1,0
240
270
300
330
360
390
Wavelength (nm)

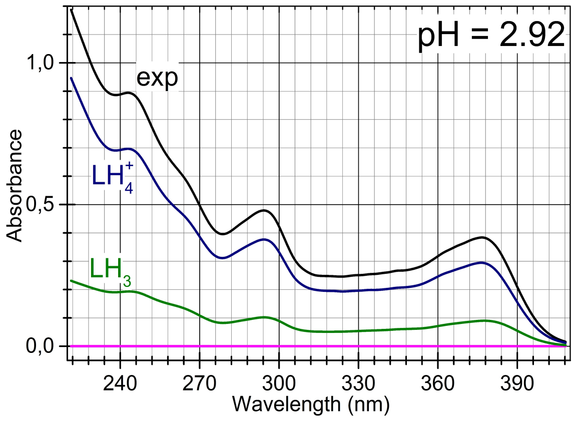
pH = 2.92
exp
LH_4^+
LH_3
Absorbance
0,0
0,5
1,0
240
270
300
330
360
390
Wavelength (nm)

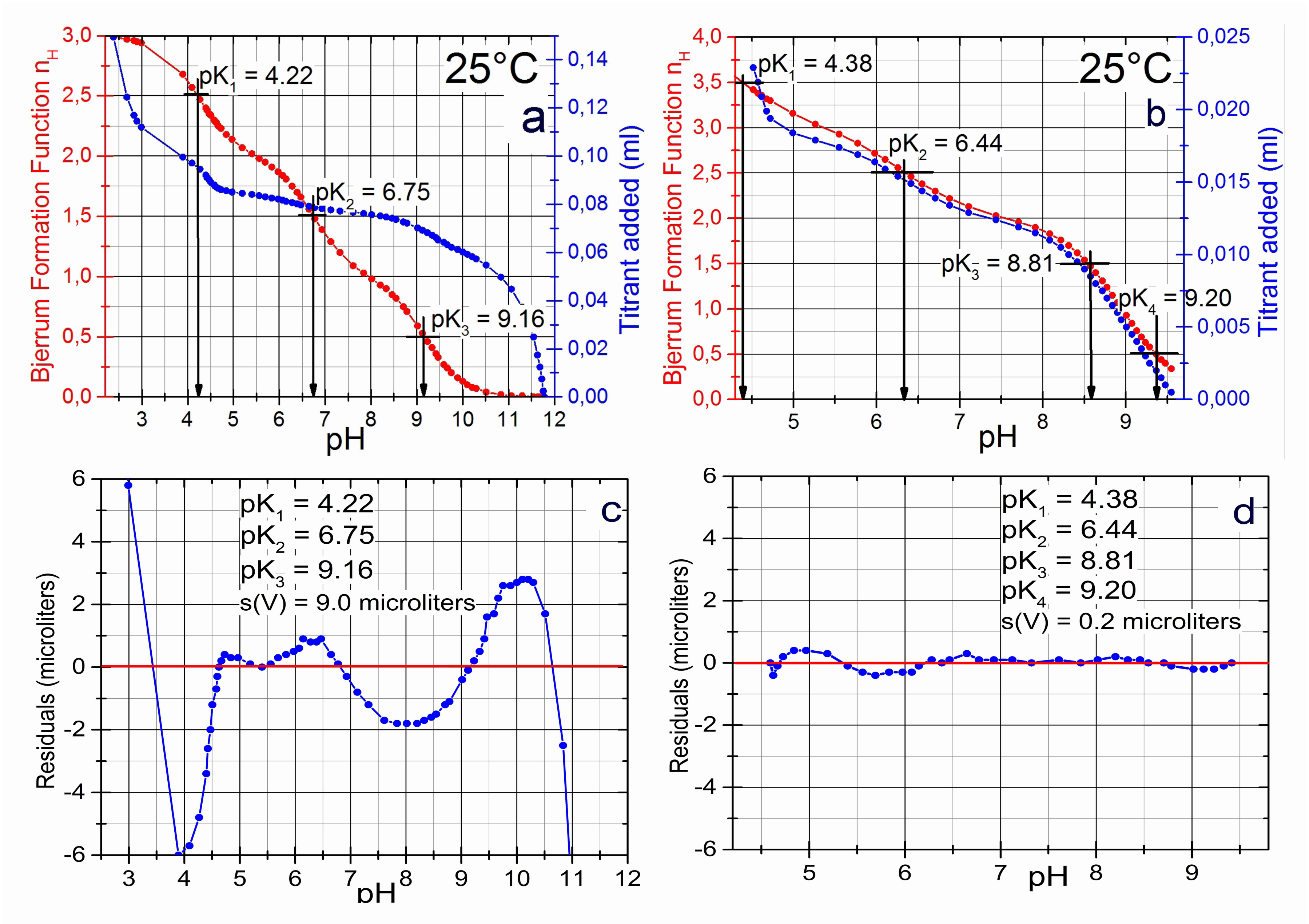
25°C
a
pK1 = 4.22
pK2 = 6.75
pK3 = 9.16
Bjerrum Formation Function nH
Titrant added (ml)
pH
25°C
b
pK1 = 4.38
pK2 = 6.44
pK3 = 8.81
pK4 = 9.20
Bjerrum Formation Function nH
Titrant added (ml)
pH
c
pK1 = 4.22
pK2 = 6.75
pK3 = 9.16
s(V) = 9.0 microliters
Residuals (microliters)
pH
d
pK1 = 4.38
pK2 = 6.44
pK3 = 8.81
pK4 = 9.20
s(V) = 0.2 microliters
Residuals (microliters)
pH

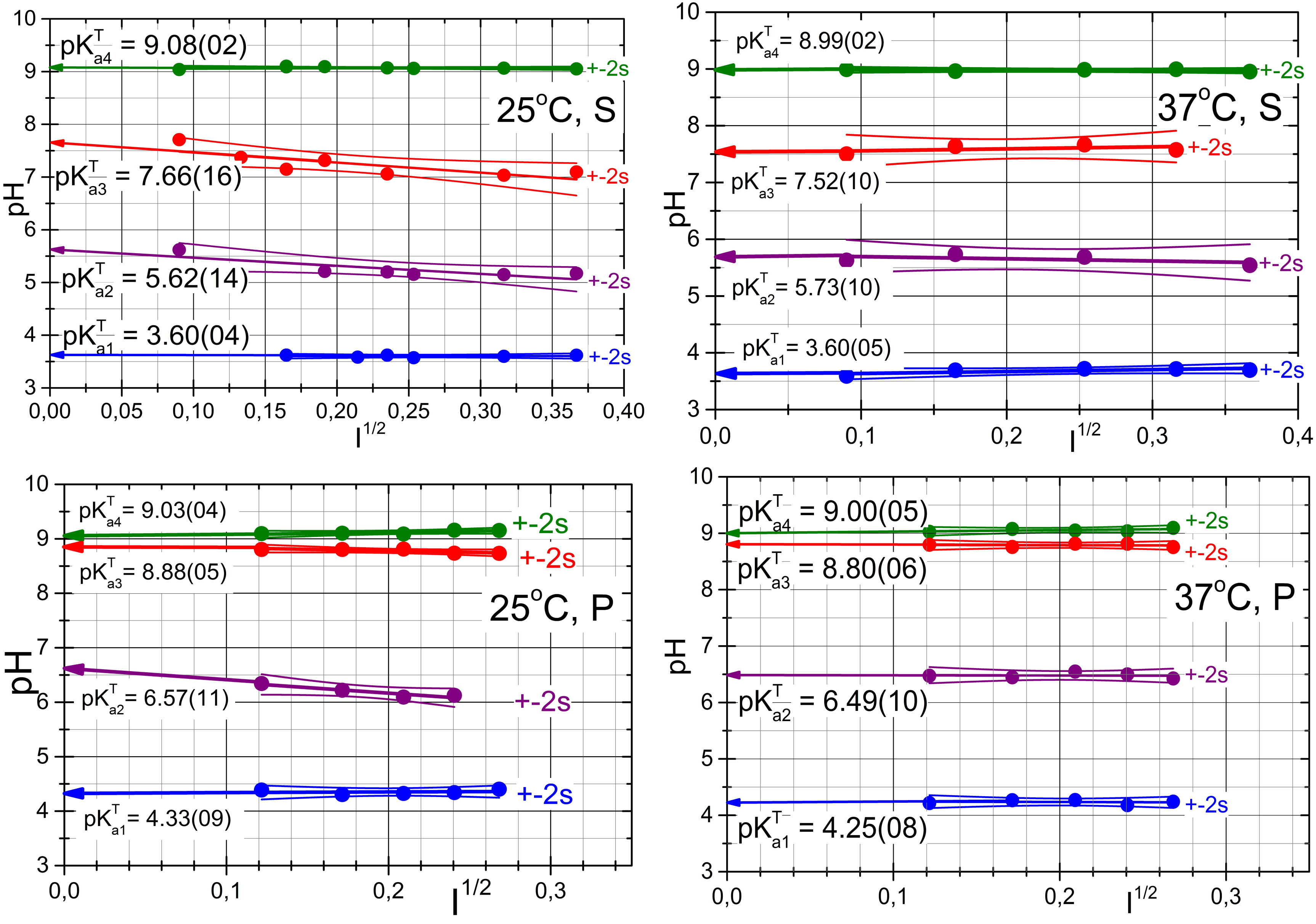
25°C, S
pK$^T_{a4}$ = 9.08(02)
pK$^T_{a3}$ = 7.66(16)
pK$^T_{a2}$ = 5.62(14)
pK$^T_{a1}$ = 3.60(04)
+-2s
pH
I$^{1/2}$
37°C, S
pK$^T_{a4}$= 8.99(02)
pK$^T_{a3}$= 7.52(10)
pK$^T_{a2}$= 5.73(10)
pK$^T_{a1}$= 3.60(05)
25°C, P
pK$^T_{a4}$= 9.03(04)
pK$^T_{a3}$= 8.88(05)
pK$^T_{a2}$= 6.57(11)
pK$^T_{a1}$= 4.33(09)
37°C, P
pK$^T_{a4}$ = 9.00(05)
pK$^T_{a3}$ = 8.80(06)
pK$^T_{a2}$ = 6.49(10)
pK$^T_{a1}$ = 4.25(08)

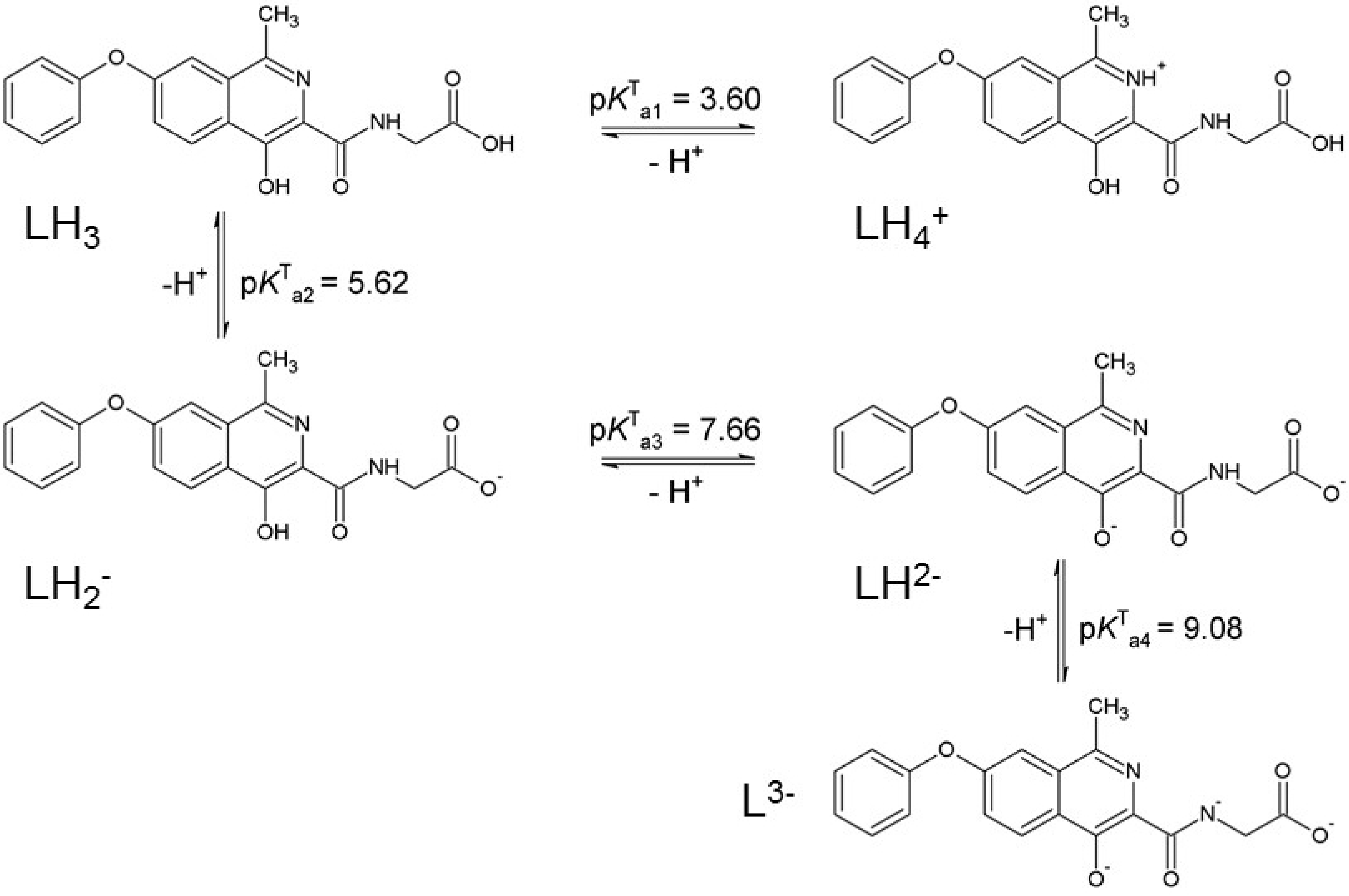
LH3
pK^T_a1 = 3.60
- H+
LH4+
-H+
pK^T_a2 = 5.62
LH2-
pK^T_a3 = 7.66
- H+
LH2-
-H+
pK^T_a4 = 9.08
L3-
CH3
O
N
NH+
NH
N-
O-
OH

Roxadustat

is hypoxia-inducible factor prolyl hydroxylase inhibitor with potencial anti-anemic activity.

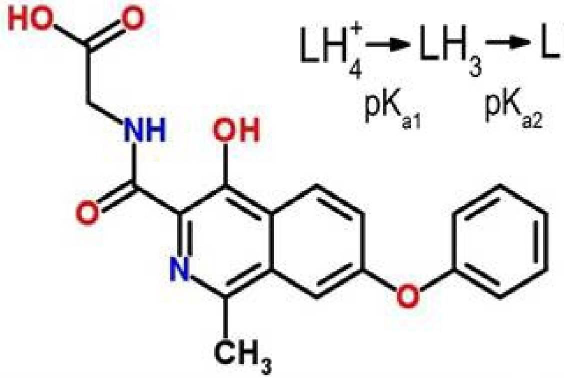

$$LH_4^+ \xrightarrow[pK_{a1}]{} LH_3 \xrightarrow[pK_{a2}]{} LH_2^- \xrightarrow[pK_{a3}]{} LH^{2-} \xrightarrow[pK_{a4}]{} L^{3-}$$

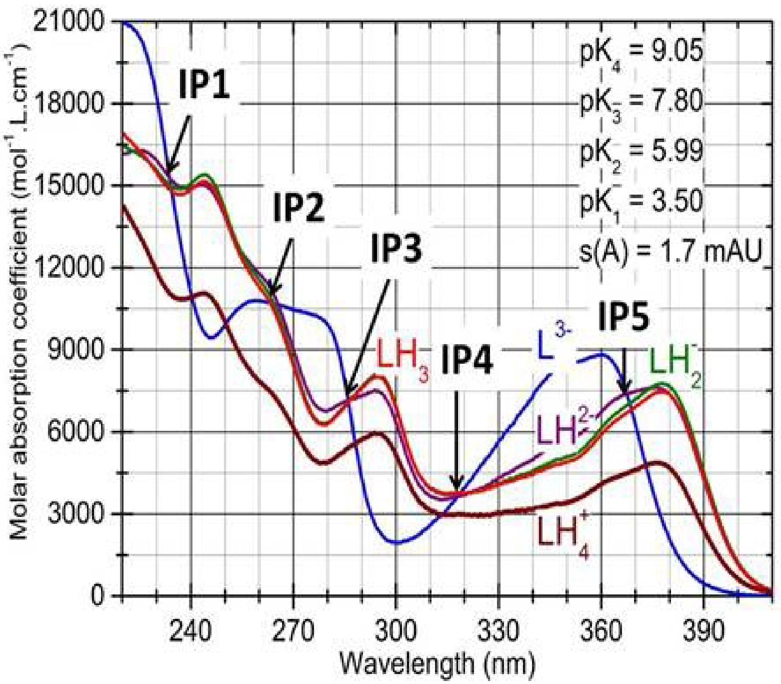

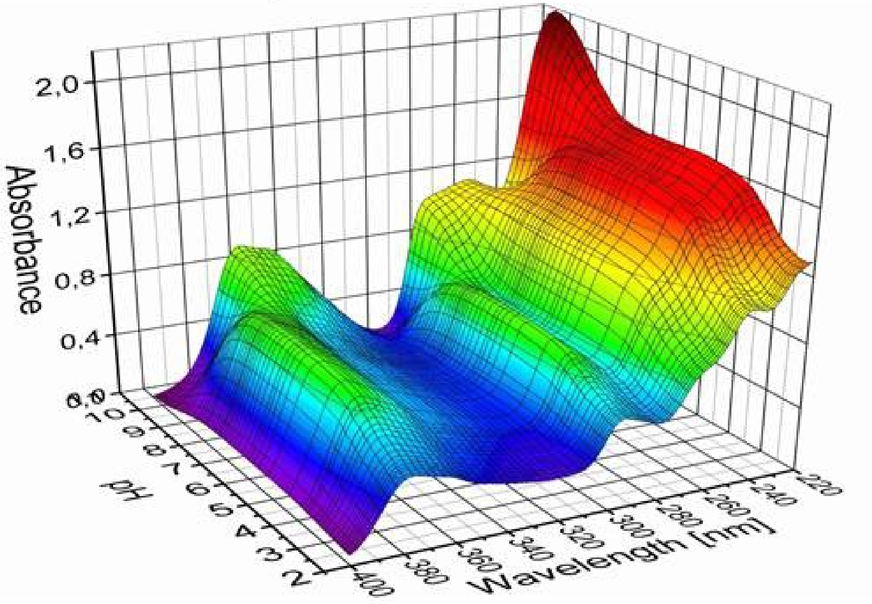

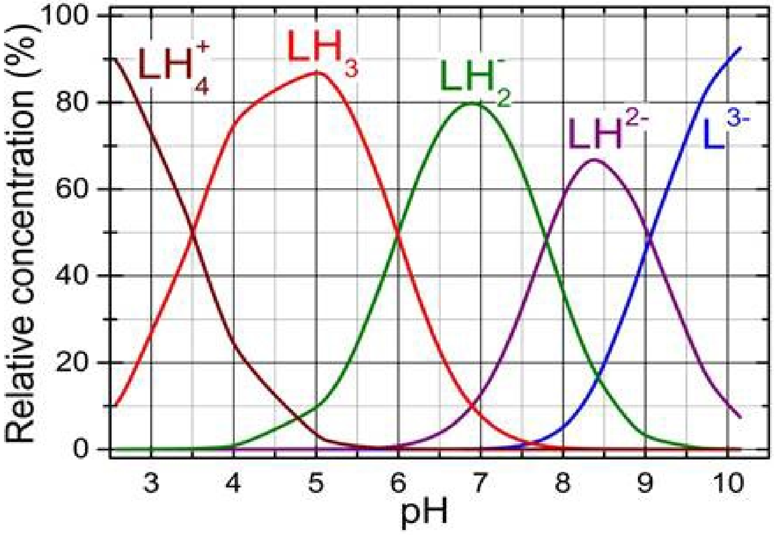

Table 1. The regression refinement of four dissociation constants p$K_{a1,}$ p$K_{a2,}$ pK_{a3} and pK_{a4} of Roxadustat with SQUAD84 and REACTLAB at 25°C and 37°C in dependence on the ionic strength. The solution of 8.0 × 10^{-5} M Roxadustat for n_s spectra measured at n_w wavelengths for n_z = 2 basic components L and H forms variously protonated species. The standard deviations of the parameter estimates are in brackets in the last valid digits. The resolution criterion and reliability of parameter estimates found were proven with goodness-of-fit statistics such as the residual standard deviation by factor analysis $s_k(A)$ [mAU] the mean residual $E|\bar{e}|$ [mAU] the standard deviation of absorbance after termination of the regression process $s(\hat{e})$ [mAU] the sigma $s(A)$ [mAU] from REACTLAB and the Hamilton R-factor of relative fitness [%] from SQUAD84.

Temperature		25°C					37°C				
Ionic strength [mol/L]		0.0081	0.0271	0.0642	0.1000	0.1345	0.0081	0.0271	0.0642	0.1000	0.1345
Cattel´s scree plot indicating the rank of the absorbance matrix (INDICES)											
Number of spectra measured, n_s		51	64	62	59	75	67	64	65	67	63
Number of wavelengths, n_w		445	445	445	445	444	222	222	222	223	222
Number of light-absorbing species, k^*		5	5	5	5	5	5	5	5	5	5
Residual standard deviation, $s_k^*(A)$ [mAU]		1.52	2.40	1.99	1.99	2.04	1.45	1.28	1.42	1.20	1.39
Estimates of dissociation constants in the searched protonation model											
pK_{a1} (s_1), LH_4^+ = $H^+ + LH_3$	SQUAD84	3.30(00)	3.45(00)	3.49(00)	3.43(00)	3.62(00)	3.59(01)	3.68(01)	3.69(01)	3.71(01)	3.70(01)
	REACTLAB	3.29(00)	3.45(00)	3.47(00)	3.42(00)	3.62(00)	3.59(00)	3.69(00)	3.72(00)	3.71(00)	3.70(00)
pK_{a2} (s_2), LH_3 = $H^+ + LH_2^-$	SQUAD84	5.69(00)	4.27(00)	4.40(00)	4.66(00)	5.17(00)	5.63(01)	5.66(01)	5.42(01)	5.96(01)	5.57(01)
	REACTLAB	5.70(01)	4.27(00)	4.41(00)	4.67(00)	5.17(00)	5.63(01)	5.74(00)	5.69(01)	5.95(00)	5.54(00)
pK_{a3} (s_3), LH_2^- = $H^+ + LH^{2-}$	SQUAD84	7.47(00)	7.19(00)	6.68(00)	6.87(00)	7.04(00)	7.50(01)	7.62(00)	7.45(00)	7.59(00)	7.36(00)
	REACTLAB	7.46(01)	6.93(00)	6.71(00)	6.87(01)	7.09(01)	7.50(01)	7.64(00)	7.66(01)	7.57(00)	7.33(00)
pK_{a4} (s_4), LH^{2-} = $H^+ + L^{3-}$	SQUAD84	9.00(00)	9.09(00)	9.05(00)	9.06(00)	9.05(00)	8.99(00)	8.96(00)	8.96(00)	8.99(00)	8.95(00)
	REACTLAB	9.01(00)	9.09(00)	9.05(00)	9.06(00)	9.05(00)	8.99(00)	8.96(00)	8.99(00)	8.99(00)	8.95(00)
Goodness-of-fit test with the statistical analysis of residuals											
Mean residual $E|\bar{e}|$ [mAU]	SQUAD84	1.11	1.77	1.47	1.45	1.51	1.03	0.95	1.02	0.89	1.04
	REACTLAB	1.14	1.79	1.51	1.47	1.53	1.05	0.99	1.06	0.92	1.06
Standard deviation of residuals $s(\hat{e})$ [mAU]	SQUAD84	1.52	2.40	1.99	1.99	2.04	1.45	2.28	1.42	1.20	1.39
	REACTLAB	1.49	2.33	1.95	1.96	2.02	1.43	1.29	1.44	1.19	1.38
Sigma from ReactLab [mAU]	REACTLAB	1.52	2.35	1.96	1.99	2.03	1.44	1.30	1.44	1.20	1.39
Hamilton R-factor from SQUAD84 [%]	SQUAD84	0.22	0.41	0.32	0.30	0.30	0.22	0.19	0.20	0.18	0.20

Table 2. ESAB regression refinement of common and group parameters for a pH-metric titration of Roxadustat titrated with HCl: the estimated dissociation constants pK_{a1}, pK_{a2}, pK_{a3} and pK_{a4} of Roxadustat in which their standard deviations are in parentheses in last valid digits. The reliability of parameter estimation is proven with a goodness-of-fit statistics: the arithmetic mean of residuals $E(\hat{e})$ [mL], the mean of absolute value of residuals, $E|\hat{e}|$ [mL], the standard deviation of residuals $s(\hat{e})$ [mL], the residual skewness $g_1(\hat{e})$ and the residual kurtosis $g_2(\hat{e})$ proving a Gaussian distribution and the Jarque-Berra normality test.
Common parameters refined: pK_{a1}, pK_{a2}, pK_{a3}, pK_{a4}. ***Group parameters refined***: H_0, L_0. ***Constants:*** $H_T = 1.0441$ mol/L, $t = 25.0$ °C, $pK_w = 13.9799$, $s(V) = s_{inst}(y) = 0.0001$ mL, I_0 adjusted (in vessel), $I_T = 0.8138$ (in burette KOH) or 1.0441 (in burette HCl).

Temperature	25°C					37°C				
Ionic strength I_0 [mol/L]	0.0148	0.0294	0.0438	0.0579	0.0719	0.0148	0.0294	0.0438	0.0579	0.0719
Estimates of the group parameters H_0 and L_0 in the searched protonation model										
Number of points used *n*	42	40	38	39	38	40	43	43	44	45
$H_0 \times$ 1E+02 [mol/L]	0.13(00)	0.13(00)	0.13(00)	0.13(00)	0.14(00)	0.13(00)	0.13(00)	0.13(00)	0.13(00)	0.13(00)
$L_0 \times$ 1E+04 [mol/L]	3.24(03)	3.34(03)	3.40(03)	3.49(03)	3.58(03)	3.34(02)	3.55(02)	3.44(03)	3.60(03)	3.47(02)
Estimates of the common parameters *i.e.* dissociation constants in the searched protonation model										
$pK_{a4}(s_4)$	9.09(02)	9.10(02)	9.09(01)	9.15(01)	9.15(02)	9.02(01)	9.07(01)	9.04(02)	9.03(02)	9.09(01)
$pK_{a3}(s_3)$	8.80(02)	8.80(02)	8.81(01)	8.73(01)	8.73(02)	8.79(01)	8.75(01)	8.81(02)	8.81(02)	8.75(01)
$pK_{a2}(s_2)$	6.34(04)	6.26(04)	6.09(04)	6.12(03)	5.70(05)	6.47(03)	6.44(02)	6.54(04)	6.49(04)	6.42(02)
$pK_{a1}(s_1)$	4.39(05)	4.30(05)	4.33(06)	4.34(05)	4.40(07)	4.21(04)	4.26(03)	4.27(07)	4.18(06)	4.24(04)
Goodness-of-fit test with the statistical analysis of residuals										
Arithmetic mean of residuals $E(\hat{e})$, [mL]	9.52E-06	-5E06	2.10E-05	1.79E-05	1.57E-05	2.5E-06	9.30E-06	-2.32E-06	3.63E-05	3.55E-05
Mean of absolute value of residuals, $E|\hat{e}|$, [mL]	0.00022	0.00025	0.00023	0.00024	0.00030	0.00023	0.00020	0.00033	0.00030	0.00022
Residual standard deviation, $s(\hat{e})$, [mL]	0.00040	0.00035	0.00033	0.00032	0.00042	0.00030	0.00028	0.00044	0.00043	0.00029
Residual skewness $g_1(\hat{e})$	-0.94	0.12	1.09	0.28	0.24	-0.48	0.28	-0.39	0.34	0.51
Residual kurtosis $g_2(\hat{e})$	8.65	4.81	5.21	4.65	4.17	2.80	3.36	2.82	3.32	3.20
Jarque-Berra test of residuals normality: *p*, Normality is	0.059, Accepted	0.888, Accepted	0.040, Rejected	0.648, Accepted	0.724, Accepted	0.341, Accepted	0.625, Accepted	0.449, Accepted	0.523, Accepted	0.283, Accepted

Table 3. Thermodynamic dissociation constants pK^{T}_{ai}, $i = 1, \ldots, 4$, at 25°C and 37°C, and thermodynamic parameters ΔH^{0}(pK^{T}_{ai}) kJ.mol^{-1}, ΔG^{0}(pK^{T}_{ai}) kJ.mol^{-1}, ΔS^{0}(pK^{T}_{ai}) J.mol^{-1}, $i = 1, \ldots, 4$ of Roxadustat.

Thermodynamic dissociation constant and thermodynamic parameters	**Spectrophotometry**		**Potentiometry**	
	25°C	**37°C**	**25°C**	**37°C**
pK^{T}_{a4}	**9.08(02)**	**8.99(02)**	**9.03(04)**	**9.00(05)**
ΔH^{0}(pK^{T}_{a4})	13.27 kJ.mol^{-1}		4.42 kJ.mol^{-1}	
ΔG^{0}(pK^{T}_{a4})	51.83 kJ.mol^{-1}	53.38 kJ.mol^{-1}	51.54 kJ.mol^{-1}	53.44 kJ.mol^{-1}
ΔS^{0}(pK^{T}_{a4})	-129.29 J.mol^{-1}	-129.29 J.mol^{-1}	-158.02 J.mol^{-1}	-158.03 J.mol^{-1}
pK^{T}_{a3}	**7.59(16)**	**7.52(10)**	**8.88(05)**	**8.80(06)**
ΔH^{0}(pK^{T}_{a3})	10.33 kJ.mol^{-1}		11.8 kJ.mol^{-1}	
ΔG^{0}(pK^{T}_{a3})	43.32 kJ.mol^{-1}	44.65 kJ.mol^{-1}	50.68 kJ.mol^{-1}	52.25 kJ.mol^{-1}
ΔS^{0}(pK^{T}_{a3})	-110.66 J.mol^{-1}	-110.66 J.mol^{-1}	-130.41 J.mol^{-1}	-130.42 J.mol^{-1}
pK^{T}_{a2}	**5.14(14)**	**5.73(10)**	**6.57(11)**	**6.49(10)**
ΔH^{0}(pK^{T}_{a2})	-87.04 kJ.mol^{-1}		11.8 kJ.mol^{-1}	
ΔG^{0}(pK^{T}_{a2})	29.34 kJ.mol^{-1}	34.02 kJ.mol^{-1}	37.50 kJ.mol^{-1}	38.53 kJ.mol^{-1}
ΔS^{0}(pK^{T}_{a2})	-390.32 J.mol^{-1}	-390.32 J.mol^{-1}	-86.19 J.mol^{-1}	-86.20 J.mol^{-1}
pK^{T}_{a1}	**3.45(04)**	**3.60(05)**	**4.33(09)**	**4.25(08)**
ΔH^{0}(pK^{T}_{a1})	-22.13 kJ.mol^{-1}		11.80 kJ.mol^{-1}	
ΔG^{0}(pK^{T}_{a1})	19.69 kJ.mol^{-1}	21.37 kJ.mol^{-1}	24.71 kJ.mol^{-1}	25.23 kJ.mol^{-1}
ΔS^{0}(pK^{T}_{a1})	-140.26 J.mol^{-1}	-140.26 J.mol^{-1}	-43.30 J.mol^{-1}	-43.31 J.mol^{-1}